

INFORMATION TO USERS

This reproduction was made from a copy of a manuscript sent to us for publication and microfilming. While the most advanced technology has been used to photograph and reproduce this manuscript, the quality of the reproduction is heavily dependent upon the quality of the material submitted. Pages in any manuscript may have indistinct print. In all cases the best available copy has been filmed.

The following explanation of techniques is provided to help clarify notations which may appear on this reproduction.

1. Manuscripts may not always be complete. When it is not possible to obtain missing pages, a note appears to indicate this.
2. When copyrighted materials are removed from the manuscript, a note appears to indicate this.
3. Oversize materials (maps, drawings, and charts) are photographed by sectioning the original, beginning at the upper left hand corner and continuing from left to right in equal sections with small overlaps. Each oversize page is also filmed as one exposure and is available, for an additional charge, as a standard 35mm slide or in black and white paper format. *
4. Most photographs reproduce acceptably on positive microfilm or microfiche but lack clarity on xerographic copies made from the microfilm. For an additional charge, all photographs are available in black and white standard 35mm slide format. *

*For more information about black and white slides or enlarged paper reproductions, please contact the Dissertations Customer Services Department.

UMI University
Microfilms
International

8601704

Wilensky, Stuart Bryan

COMPLEX FORMATION BETWEEN 2-POLYVINYLPYRIDINE AND IODINE IN
SOLUTION AND IN THE SOLID-STATE

City University of New York

Ph.D. 1985

**University
Microfilms
International**

300 N. Zeeb Road, Ann Arbor, MI 48106

**COMPLEX FORMATION BETWEEN 2-POLYVINYLPYRIDINE
AND IODINE IN SOLUTION AND IN THE SOLID-STATE**

BY

STUART BRYAN WILENSKY

A dissertation submitted to the Graduate Faculty
in Chemistry in partial fulfillment of the requirements
for the degree of Doctor of Philosophy
The City University of New York

1985

This manuscript has been read and accepted for the Graduate Faculty in Chemistry in satisfaction of the dissertation requirement for the degree of Doctor of Philosophy.

6/7/85
date

Seymour Aronson
Chairman of Examining Committee

6/7/85
date

A.M. [Signature]
Executive Officer

Fitzgerald B. Bramwell

Jack Morrow

Grace M. Wieder

Supervisory Committee

The City University of New York

ABSTRACT

COMPLEX FORMATION BETWEEN 2-POLYVINYLPYRIDINE AND IODINE IN SOLUTION AND IN THE SOLID-STATE

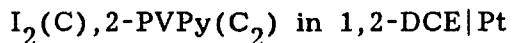
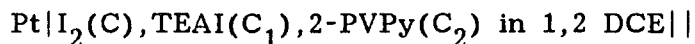
by

STUART BRYAN WILENSKY

ADVISOR: PROFESSOR SEYMOUR ARONSON

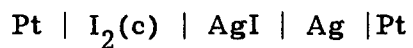
A study was made on the ionic equilibria of 2-polyvinylpyridine(2-PVPy) and iodine, and pyridine(Py) and iodine in 1,2-dichloroethane. A significant difference was found between freshly prepared and stored solutions. Experimental data for the stored solutions were reproducible and consistent.

EMF measurements on cells of the type



where TEAI is tetraethylammonium iodide, were performed. For the proposed dissociation of the molecular complex, the degree of ionization and the equilibrium constant were calculated. Conductivity and concentration cell measurements yielded additional information. Solutions of Py-I_2 as well as solutions of 2-PVPy-I_2 were studied.

Solid-state samples of iodine complexed with 2-PVPy, pyrolyzed polyacrylonitrile, pyrene, and perylene were examined. EMF data on solid-state cells of the type



where $\text{I}_2(\text{c})$ represents pure or complexed iodine, were obtained. The thermodynamic activity of iodine as a function of iodine content was determined. Results indicate that the chemical bonding between iodine and the polymer is relatively weak. Electrical conductivity data show a strong dependence of conductivity on the iodine content of the complex. Electron spin resonance spectra have been collected to further characterize the systems.

ACKNOWLEDGMENTS

I wish to express my most sincere thanks to my mentor, Professor Seymour Aronson, who shared his time and invaluable knowledge with me. His guidance and infinite patience have made this project possible.

No less important is my wife, Dawn, who always encouraged me and had unlimited confidence in me. She is my inspiration.

I would like to thank my parents for all their support and guidance and for molding me into the person I am today.

I also wish to thank my thesis committee, Professors Fitzgerald B. Bramwell, Jack Morrow, and Grace M. Wieder for their contributions of time and advice throughout the course of this research.

It is a pleasure to acknowledge the glassblower, Mr. Ottmar Safferling, who with the utmost skill, prepared all my specialty glassware and would drop everything to make an emergency repair for me.

A special thanks to Professor Henry Teoh, who spent a great deal of time developing a technique for measuring the electrical conductivity of my solid-state samples and made the electrical conductivity measurements on my solid-state samples.

Finally, my thanks and best wishes to my colleagues and members of the Chemistry Faculty as well as many people from other disciplines who supplied advice and helped make my graduate years so pleasurable. I will long remember you.

STUART BRYAN WILENSKY

CONTENTS

ABSTRACT	iii
ACKNOWLEDGMENTS	v
LIST OF TABLES	ix
LIST OF FIGURES	xi
Chapter 1:	
INTRODUCTION	1
Chapter 2:	
EXPERIMENTAL	4
Chemicals	4
Preparation of iodinated solid samples	10
Electrochemical Measurements on solid-state samples	12
Spectral Measurements	14
Electrochemical and Conductivity Measurements on Solutions	14
Chapter 3:	
Complexes of Pyridine and Polyvinylpyridine in Solution	17
Equilibrium Constants for Complexation	17
Electrochemical Measurements in Solution	23
Ultraviolet-Visible Spectroscopy	36
Conductivity Measurements	39

I ₂ Concentration Cell Measurements	45
2-Polyvinylpyridine-Iodine and other solid-state	
complexes	49
Electrochemical Measurements	49
Electrical Conductivity Measurements	56
Electron Spin Resonance	60
APPENDIX A EMF data on 2-polyvinylpyridine-iodine in	
1,2 dichloroethane solutions	65
APPENDIX B EMF data on pyridine-iodine in	
1,2 dichloroethane solutions	70
REFERENCES	75

LIST OF TABLES

<u>Table</u>	<u>Page</u>
1. Equilibrium constants of formation of PyI_2 and 2-PVPyI_2 ...	22
2. EMF data on the cell $\text{Pt} \text{I}_2(2.030 \times 10^{-3}\text{M}), \text{TEAI}(\text{C}_1, \text{M}), 2\text{-PVPy}(.2034\text{M}) $ $\text{I}_2(2.030 \times 10^{-3}\text{M}), 2\text{-PVPy}(.2034\text{M}) \text{Pt}$	30
3. EMF data on the cell $\text{Pt} \text{I}_2(2.000 \times 10^{-3}\text{M}), \text{TEAI}(\text{C}_1, \text{M}), \text{Py}(.1986\text{M}) $ $\text{I}_2(2.000 \times 10^{-3}\text{M}), \text{Py}(.1986\text{M}) \text{Pt}$	31
4. Summary of data from electrochemical cells of the type described by Line Diagram 7 for 2-PVPy-I_2	34
5. Summary of data from electrochemical cells of the type described by Line Diagram 7 for Py-I_2	35
6. Summary of data from conductivity cells of 2-PVPy-I_2	40
7. Summary of data from conductivity cells of Py-I_2	41
8. EMF data on cells of the type $\text{Pt} \text{I}_2(\text{C}_1, \text{M}), \text{X}(\text{C}, \text{M})$ in 1,2-DCE $\text{I}_2(\text{C}_2, \text{M}), \text{X}(\text{C}_3, \text{M})$ in 1,2-DCE Pt X=Py	47
9. EMF data on cells of the type $\text{Pt} \text{I}_2(\text{C}_1, \text{M}), \text{X}(\text{C}, \text{M})$ in 1,2-DCE $\text{I}_2(\text{C}_2, \text{M}), \text{X}(\text{C}_3, \text{M})$ in 1,2-DCE Pt X=2-PVPy	48
10. Comparison of free energies of formation of iodine complexes	54
11. EMF data on the cell $\text{Pt} \text{I}_2(2.708 \times 10^{-4}\text{M}), \text{TEAI}(\text{C}_1, \text{M}), 2\text{-PVPy}(2.536 \times 10^{-2}\text{M}) $ $\text{I}_2(2.708 \times 10^{-4}\text{M}), 2\text{-PVPy}(2.536 \times 10^{-2}\text{M}) \text{Pt}$	66

12. EMF data on the cell
 $\text{Pt}|\text{I}_2(5.165 \times 10^{-4}\text{M}), \text{TEAI}(\text{C}_1, \text{M}), 2\text{-PVPy}(4.968 \times 10^{-2}\text{M})||$
 $\text{I}_2(5.165 \times 10^{-4}\text{M}), 2\text{-PVPy}(4.968 \times 10^{-2}\text{M})|\text{Pt} \dots\dots\dots 67$
13. EMF data on the cell
 $\text{Pt}|\text{I}_2(1.112 \times 10^{-3}\text{M}), \text{TEAI}(\text{C}_1, \text{M}), 2\text{-PVPy}(.1000\text{M})||$
 $\text{I}_2(1.112 \times 10^{-3}\text{M}), 2\text{-PVPy}(.1000\text{M})|\text{Pt} \dots\dots\dots 68$
14. EMF data on the cell
 $\text{Pt}|\text{I}_2(2.963 \times 10^{-3}\text{M}), \text{TEAI}(\text{C}_1, \text{M}), 2\text{-PVPy}(.2979\text{M})||$
 $\text{I}_2(2.963 \times 10^{-3}\text{M}), 2\text{-PVPy}(.2979\text{M})|\text{Pt} \dots\dots\dots 69$
15. EMF data on the cell
 $\text{Pt}|\text{I}_2(2.558 \times 10^{-4}\text{M}), \text{TEAI}(\text{C}_1, \text{M}), \text{Py}(2.483 \times 10^{-2}\text{M})||$
 $\text{I}_2(2.558 \times 10^{-4}\text{M}), \text{Py}(2.483 \times 10^{-2}\text{M})|\text{Pt} \dots\dots\dots 71$
16. EMF data on the cell
 $\text{Pt}|\text{I}_2(4.920 \times 10^{-4}\text{M}), \text{TEAI}(\text{C}_1, \text{M}), \text{Py}(4.965 \times 10^{-2}\text{M})||$
 $\text{I}_2(4.920 \times 10^{-4}\text{M}), \text{Py}(4.965 \times 10^{-2}\text{M})|\text{Pt} \dots\dots\dots 72$
17. EMF data on the cell
 $\text{Pt}|\text{I}_2(1.012 \times 10^{-3}\text{M}), \text{TEAI}(\text{C}_1, \text{M}), \text{Py}(9.931 \times 10^{-2}\text{M})||$
 $\text{I}_2(1.012 \times 10^{-3}\text{M}), \text{Py}(9.931 \times 10^{-2}\text{M})|\text{Pt} \dots\dots\dots 73$
18. EMF data on the cell
 $\text{Pt}|\text{I}_2(2.980 \times 10^{-3}\text{M}), \text{TEAI}(\text{C}_1, \text{M}), \text{Py}(.2972\text{M})||$
 $\text{I}_2(2.980 \times 10^{-3}\text{M}), \text{Py}(.2972\text{M})|\text{Pt} \dots\dots\dots 74$

LIST OF FIGURES

<u>Figure</u>	<u>Page</u>
1. Structures of pyridine and 2-polyvinylpyridine	7
2. Structures of pyrene and perylene	8
3. Structures of polyacrylonitrile and pyrolyzed polyacrylonitrile	9
4. Apparatus for preparation of iodinated samples	11
5. Cell for electrochemical measurements of solid-state samples .	13
6. Cell for electrochemical measurements of solutions	16
7. Visible spectra of $9.068 \times 10^{-4} \text{M}$ iodine with various concentrations of 2-PVPy in benzene	19
8. $[1/(\epsilon_{I_2} - \epsilon_t)] \times 10^3$ vs $1/C_d$ for $9.068 \times 10^{-4} \text{M}$ I_2 with various 2-PVPy concentrations in benzene	20
9. $[1/(\epsilon_{I_2} - \epsilon_t)] \times 10^3$ vs $1/C_d$ for $9.113 \times 10^{-4} \text{M}$ I_2 with various Py concentrations in benzene	21
10. Variation of percent ionization of 2-PVPy I_2 and Py I_2 with time in 1,2-DCE	29
11. EMF data on the cell Pt $ I_2(2.030 \times 10^{-3} \text{M}), TEAI(C_1, \text{M}), 2\text{-PVPy}(.2034\text{M}) $ $I_2(2.030 \times 10^{-3} \text{M}), 2\text{-PVPy}(.2034\text{M}) Pt$	32
12. EMF data on the cell Pt $ I_2(2.000 \times 10^{-3} \text{M}), TEAI(C_1, \text{M}), Py(.1986\text{M}) $ $I_2(2.000 \times 10^{-3} \text{M}), Py(.1986\text{M}) Pt$	33
13. Variation of molar absorptivity of Py- I_2 and 2-PVPy- I_2 at 365nm with time	38
14. Variation of specific conductivity with iodine concentration and storage time for 2-PVPy- I_2 solutions	42

15. Variation of specific conductivity with iodine concentration and storage time for Py-I ₂ solutions	43
16. Variation of specific conductivity with iodine concentration for 2-PVPy-I ₂ and Py-I ₂ solutions stored four weeks	44
17. Variation of solid-state cell voltage with iodine content	53
18. Variation of solid-state cell voltage with iodine content for 2-PVPy and PPAN-1	55
19. Variation of conductivity with iodine content for PPAN	57
20. Variation of conductivity with iodine content for 2-PVPy	58
21. Comparison of the conductivity of PPAN using two different doping procedures	59
22. Electron spin resonance spectrum of PPAN-1(I ₂) _{0.5}	61
23. Electron spin resonance spectrum of 2-PVPy(I ₂) _{1.1} 90°C anneal	62
24. Variation of the g-factor with iodine content for 2-PVPy	63
25. Variation of the g-factor with iodine content for PPAN-1	64

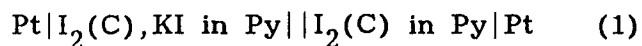
Chapter 1

INTRODUCTION

During the past twenty years, a great deal of information has been produced on molecular charge transfer complexes, including a number of papers on the pyridine-iodine molecular complex. Solutions of iodine dissolved in pyridine have electrical conductivities similar to those of aqueous salt solutions. The ionic nature of these solutions has been the focus of much investigation¹⁻⁷.

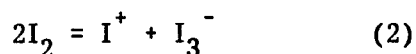
Little attention has been paid to pyridine-iodine (Py-I₂) complex formation in mixed solvents of pyridine with other organic liquids. No investigations have been made comparing the Py-I₂ system and the polyvinylpyridine-iodine (PVPy-I₂) system. Such a comparison performed in some common solvent could prove interesting. In addition, comparison of these systems with Py-I₂ in pure pyridine might help answer some long standing questions on the pyridine-iodine complexation that are still not resolved.

In a recent investigation, Aronson et al⁸ obtained information on ionic equilibria in fresh Py-I₂ solutions with high iodine concentrations using electrochemical cell measurements. Electrochemical cells of the type



were utilized, where C represents the nominal concentration of elemental iodine in pyridine. A simple mechanism for the ionization

of PyI_2 molecular complex which was previously proposed^{1,3,6,7} was applied.

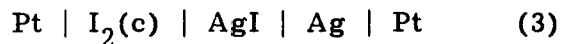


I_2 in Reaction 2 is most likely totally in the molecular complex form PyI_2 . The cation, I^+ , may be in the form Py_2I^+ or PyI^+ , with the former most likely present in pure pyridine.

Results have indicated that 8%-18% ionization of the PyI_2 occurs. Values of the equilibrium constant of Reaction 2 ranging from 2×10^{-3} to 1×10^{-2} are reported. Modification of the proposed mechanism may be necessary as indicated by the variation of the equilibrium constant.

In this study, we employed the same type of electrochemical cell measurements in studying ionic equilibria of 2-polyvinylpyridine-iodine (2-PVPy-I_2) in 1,2 dichloroethane (1,2-DCE). Comparable solutions of Py-I_2 in 1,2-DCE have also been studied. A significant difference is found between fresh and stored solutions of 2-PVPy-I_2 and Py-I_2 in 1,2-DCE. For stored solutions the experimental data are consistent and reproducible. Results indicate that 23%-24% ionization of PyI_2 and 2-PVPyI_2 occurs and that the value of the equilibrium constant for Reaction 2 is 2×10^{-2} to 3×10^{-2} . Studies of conductivity, ultraviolet-visible spectroscopy and iodine concentration cell measurements have yielded some additional information.

We have also studied the 2-PVPy-I₂ complex in the solid-state. We have used solid-state electrochemical cells of the type



in obtaining information on the thermodynamic activity of iodine in the complex. Comparison of this data has been made to similar measurements on other iodine charge transfer complexes, including pyrolyzed polyacrylonitrile (PPAN). A similar feature of the structure of PPAN and 2-PVPy is that the nitrogen atoms form part of an alternating system of double and single bonds. In the case of 2-PVPy the alternation occurs only in the individual pyridyl groups.

The thermodynamic data obtained is consistent with previously reported data available on some of the iodine charge transfer complex systems studied. Electrical conductivity data and electron spin resonance data have also been obtained.

Chapter 2

EXPERIMENTAL

2.1 CHEMICALS

Materials were prepared and purified as follows:

Fisher certified ACS grade pyridine was allowed to stand over solid potassium hydroxide for several days, then refluxed over calcium hydride for several hours, and then repeatedly distilled from fresh portions of the hydride with a boiling point 115-116 °C at 760 torr. This procedure sufficed to give a highly purified and anhydrous pyridine whose specific conductivity was below $1 \times 10^{-7} \text{ (ohm-cm)}^{-1}$.

Fisher certified ACS grade benzene and orthodichlorobenzene were each stirred with concentrated sulfuric acid, washed repeatedly with water and distilled from barium oxide. The boiling point of purified benzene was 80.0-80.5 °C . The boiling point of purified orthodichlorobenzene was 181-182 °C at 760 torr.

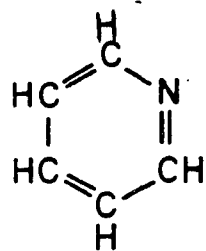
Fisher certified ACS grade 1,2-dichloroethane was dried over calcium hydride for several days, then refluxed over calcium hydride for one day and repeatedly distilled from fresh portions of this hydride. A middle fraction was collected. This gave a pure, anhydrous product with a normal boiling point of 82.9-83.1 °C .

Fisher laboratory grade resublimed iodine was resublimed twice and kept in a desiccator over anhydrous copper sulfate until used.

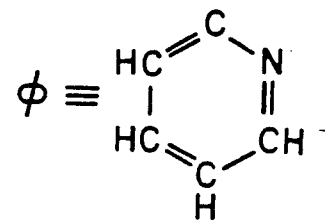
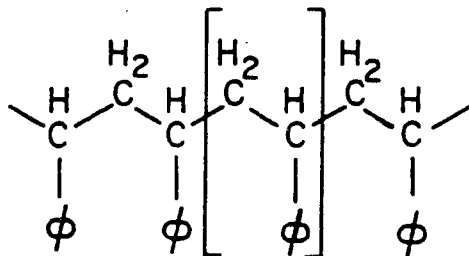
Graphite powder, SP-1 grade, was purchased from The National Carbon Company (Union Carbide). Tetraethylammonium iodide, silver iodide, and powdered silver metal were obtained in high purity from Alfa Chemicals.

The chemicals pyrene (Pyr), perylene (Pe), polyacrylonitrile (PAN) and 2-polyvinylpyridine (2-PVPy) were obtained in the highest commercial grades available from Aldrich Chemical Company. Structures of these substances are presented in Figures 1, 2 and 3. PAN was heated in a sealed, evacuated Pyrex tube for seven days at 180 °C and was subsequently heated in a pumping vacuum at 250 °C for six hours. This material we designated as PPAN-1. A portion of the PPAN-1 was further heated in a pumping vacuum at 350 °C for three hours and is designated as PPAN-2. Elemental analysis on PPAN-2 and PPAN-1 samples were performed by Schwarzkopf Microanalytical Laboratory of Woodside, New York. The compositions of PPAN-1 and PPAN-2 were found to be $C_3H_3N_{0.99}$ and $C_3H_{2.44}N_{0.90}$ respectively. Spectra of PPAN-1 and PPAN-2 obtained on a Perkin Elmer Model 267 Grating Infrared Spectrophotometer showed the absorption peaks corresponding to cyclized PAN⁹. The peaks for PPAN-2 were generally broader. We can conclude from the data that PPAN-1 and PPAN-2 are primarily

cyclized PAN. PPAN-2 has been degraded somewhat by treatment at the higher temperature, resulting in a loss of nitrogen and hydrogen.

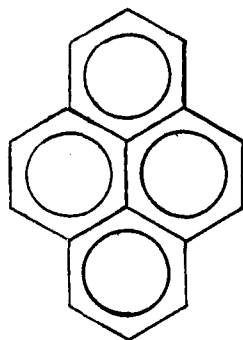
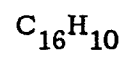


PYRIDINE

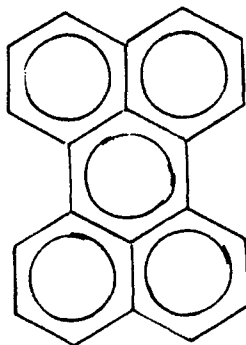
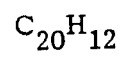


2-POLYVINYLPIRIDINE

Figure 1: Structures of pyridine(Py) and 2-polyvinylpyridine(2-PVPy)

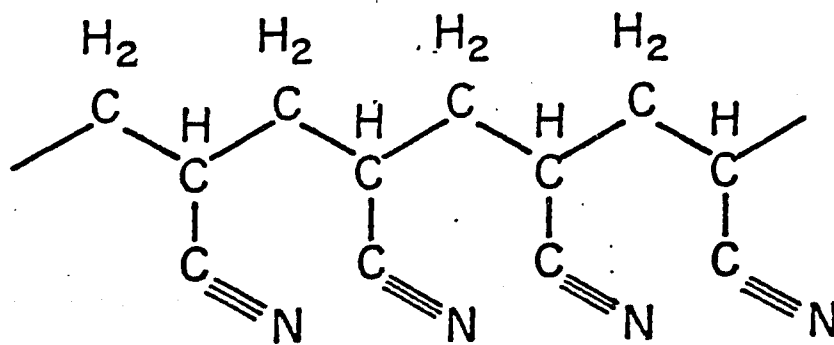


PYRENE

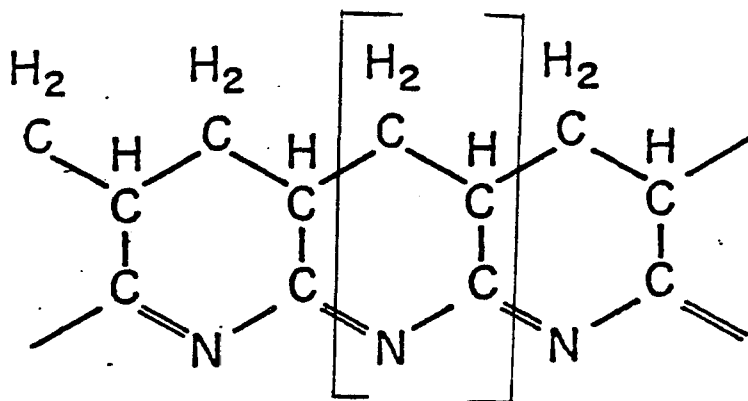


PERYLENE

Figure 2: Structures of pyrene(Pyr) and perylene(Pe)



POLYACRYLONITRILE



PYROLYZED POLYACRYLONITRILE

Figure 3: Structures of polyacrylonitrile (PAN) and pyrolyzed polyacrylonitrile(PPAN-1)

2.2 PREPARATION OF IODINATED SOLID SAMPLES

Preliminary information on the uptake of iodine by PPAN-1, PPAN-2 and 2-PVPy was obtained by enclosing samples of each in evacuated Pyrex tubes with iodine at 90 °C for 48 hours. The polymer and iodine were in contact only through the vapor phase. The experimental cell set up is pictured in Figure 4. The amount of iodine absorbed (moles of I₂ per mole repeating polymer unit), as measured by weight increase, was 0.9-1.0 for PPAN-1, 1.0-1.1 for PPAN-2 and 2.20-2.40 for 2-PVPy.

Designated compositions of Pyrene-I₂, Perylene-I₂, PPAN-1-I₂ and PPAN-2-I₂ were prepared by mixing weighed amounts of iodine and organic substances, and annealing in sealed, evacuated tubes for 48 hours at 90 °C. In the case of 2-PVPy-I₂, the iodine-polymer mixtures were annealed either at 50 °C for four days, 70 °C for three days, 90 °C for two days or 150 °C for one day.

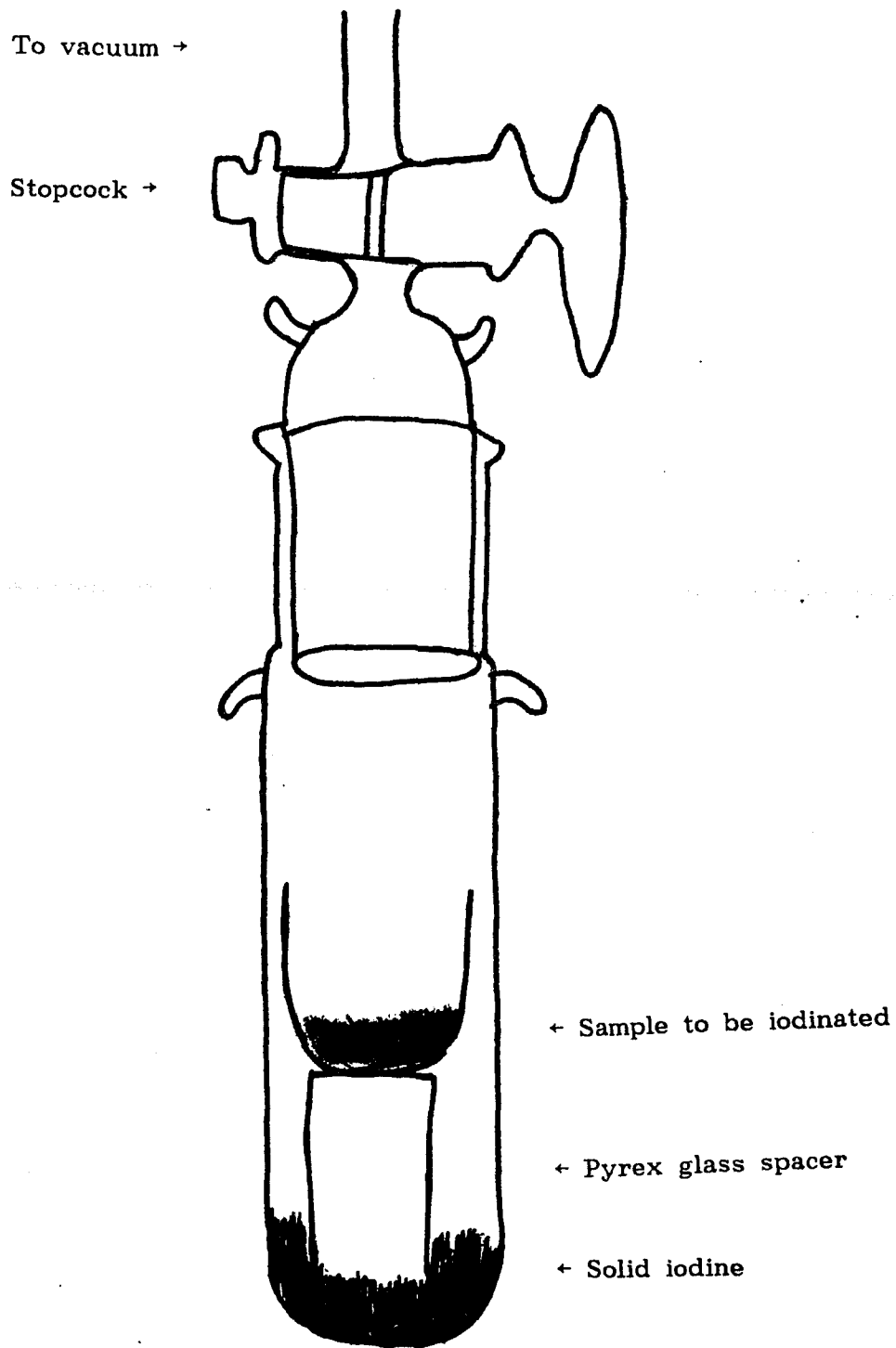


Figure 4: Apparatus for the preparation of iodinated samples

2.3 ELECTROCHEMICAL MEASUREMENTS ON SOLID-STATE SAMPLES

For the electrochemical cell measurements, a sample of powdered iodine, or iodinated hydrocarbon or polymer was mixed with graphite and was pressed into a pellet using a Parr pellet press. The graphite served as an inert, electrically conducting medium. The electrochemical cells were assembled in two parts. A layer of silver iodide powder was pressed on top of a layer of pressed silver powder. The iodinated polymer or hydrocarbon pellet was placed on top of the Ag-AgI pellet and the two pellets were compressed by springs between pieces of platinum foil attached to platinum leads. The cell is pictured in Figure 5. EMF measurements at room temperature were made using a Keithley 602 electronic multimeter. Readings on a sample were continued until steady readings were obtained for a half hour. Measurements with varying amounts of graphite mixed with the organic component confirmed that the voltage measured was independent of graphite content, within wide limits. The reproducibility of voltage readings, taking into account day-to-day voltage changes on the same sample, and variations from sample to sample of the same composition prepared separately was generally within $\pm 10\text{mV}$.

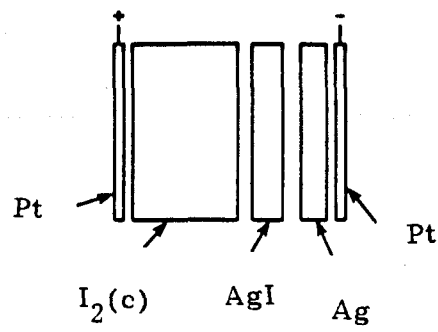


Figure 5: Cell for electrochemical measurements on solid-state samples

2.4 SPECTRAL MEASUREMENTS

Ultraviolet-visible absorption measurements on liquid samples were made with a Cary 17 spectrophotometer using clear, quartz cells of 10mm and 2mm thickness.

Electron spin resonance spectra were obtained on a Varian Model E-9 Electron Spin Resonance Spectrometer using 4mm, quartz ESR tubes.

2.5 ELECTROCHEMICAL AND CONDUCTIVITY MEASUREMENTS ON SOLUTIONS

The electrochemical measurements were made in a 2-compartment "H" cell in which separation of the compartments was effected by a fine-frit disk. Both compartments were filled to the same level. Pieces of platinum foil attached to platinum wire leads were inserted into each compartment to serve as electrodes. Voltage measurements were made with a Keithley Model 160B digital multimeter. The cell design is shown in Figure 6. All measurements were made in a constant temperature water bath regulated to 25.0 ± 0.1 °C .

Conductivity measurements were made using a standard conductivity cell with platinum electrodes and a YSI Model 31 conductivity bridge. The cell constant was determined to be

0.1037cm^{-1} using a 0.02000 Normal solution of potassium chloride at $25.0\text{ }^{\circ}\text{C}$.

The platinum electrodes and cells were cleaned by immersion in hot concentrated nitric acid, and then in cleaning solution for several days. The electrodes were then repeatedly rinsed with distilled water and left standing in distilled water for several days.

All solutions of iodine and pyridine and iodine and polyvinylpyridine were prepared just before the first measurement of a property. Measurements of that property were taken for fresh solutions and then made at intervals of one day, three to four days, one week, two weeks, three weeks, etc., for a total time of one month. All stored solutions were protected by sealing flasks with Parafilm (American Can Company).

The term "nominal concentration" when used in conjunction with either I_2 or tetraethylammonium iodide is the number of moles of I_2 or tetraethylammonium iodide added to a liter of solution. The dissociation and interactions of I_2 and tetraethylammonium iodide in solution are not included.

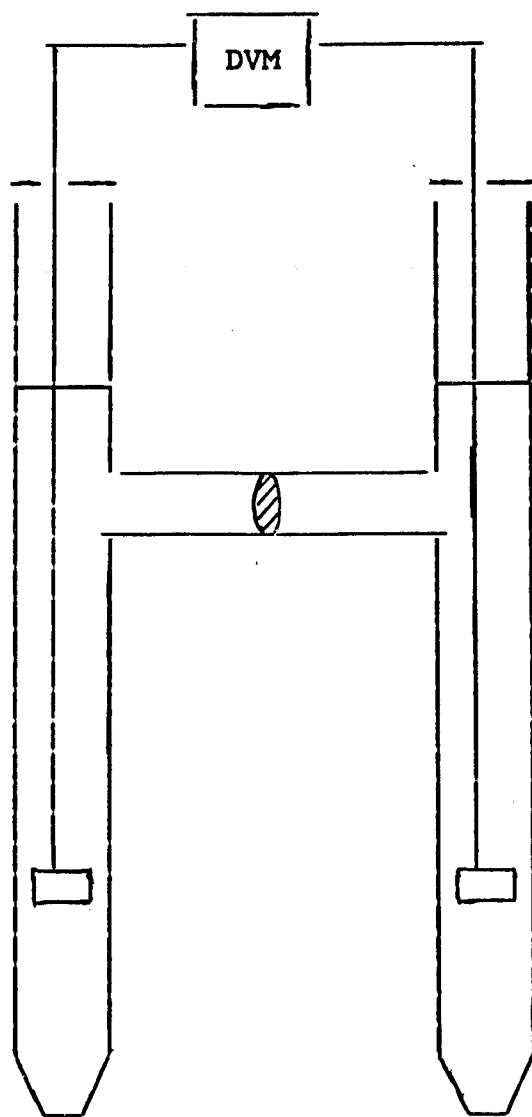


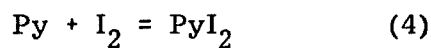
Figure 6: Cell for electrochemical measurements of solutions

Chapter 3

3.1 COMPLEXES OF PYRIDINE AND POLYVINYLPIRIDINE IN SOLUTION

3.1.1 Equilibrium Constants for Complexation

The complexation of pyridine by iodine may be written



The equilibrium constant for this reaction may be written

$$K_{\text{eq}} = [\text{PyI}_2]/[\text{Py}][\text{I}_2] \quad (5)$$

Analogous expressions may be written for the formation of 2-PVPyI₂.

Sets of solutions were prepared, each having the same initial iodine concentration, approximately 9×10^{-4} M. The concentration of pyridine or 2-polyvinylpyridine was then varied in each solution, ranging from 2×10^{-3} M to 4.5×10^{-2} M. The visible spectra of each of these solutions was then obtained. The results of such an experiment for 2-PVPy-I₂ in benzene is shown in Figure 7. Similar sets of spectra are obtained for solutions of Py-I₂ in benzene. Spectra of freshly made solutions of Py-I₂ and 2-PVPy-I₂ in 1,2 dichloroethane or orthodichlorobenzene appear qualitatively similar to those obtained in benzene.

We have used the technique of McKinley et al¹⁰, who made use of the Ketelaar equation to determine equilibrium constants.

$$1/[\epsilon_{\text{I}_2} - \epsilon_t] = [1/C_d][1/K_{\text{eq}}[\epsilon_{\text{I}_2} - \epsilon_c]] + 1/[\epsilon_{\text{I}_2} - \epsilon_c] \quad (6)$$

where

ϵ_t = apparent molar absorptivity of I_2

ϵ_c and ϵ_{I_2} = molar absorptivities of the complex and I_2 respectively

K_{eq} = equilibrium constant of complexation

C_d = concentration of pyridine or 2-polyvinylpyridine

A plot of $1/[\epsilon_{I_2} - \epsilon_t]$ vs $1/C_d$ gives a straight line. From the slope and intercept a value of K_{eq} is determined. Examples of these plots are shown in Figures 8 and 9.

Equilibrium constants of formation for PyI_2 and $2-PVPI_2$ were determined in benzene, 1,2 dichloroethane, and orthodichlorobenzene. A least squares analysis was employed to determine the y-intercepts and the slopes. The formation constants obtained are presented in Table 1.

Almost identical values of K_{eq} for PyI_2 and $2-PVPI_2$ are obtained in benzene. K_{eq} values for PyI_2 in each of the other two solvents are double the values for $2-PVPI_2$.

$$a \equiv I_2 = 9.068 \times 10^{-4} \text{ M } 2\text{-PVPy} = 4.526 \times 10^{-2} \text{ M}$$

$$b \equiv I_2 = 9.068 \times 10^{-4} \text{ M } 2\text{-PVPy} = 2.263 \times 10^{-2} \text{ M}$$

$$c \equiv I_2 = 9.068 \times 10^{-4} \text{ M } 2\text{-PVPy} = 1.584 \times 10^{-2} \text{ M}$$

$$d \equiv I_2 = 9.068 \times 10^{-4} \text{ M } 2\text{-PVPy} = 9.053 \times 10^{-3} \text{ M}$$

$$e \equiv I_2 = 9.068 \times 10^{-4} \text{ M } 2\text{-PVPy} = 4.526 \times 10^{-3} \text{ M}$$

$$f \equiv I_2 = 9.068 \times 10^{-4} \text{ M } 2\text{-PVPy} = 2.263 \times 10^{-3} \text{ M}$$

$$g \equiv I_2 = 9.068 \times 10^{-4} \text{ M}$$

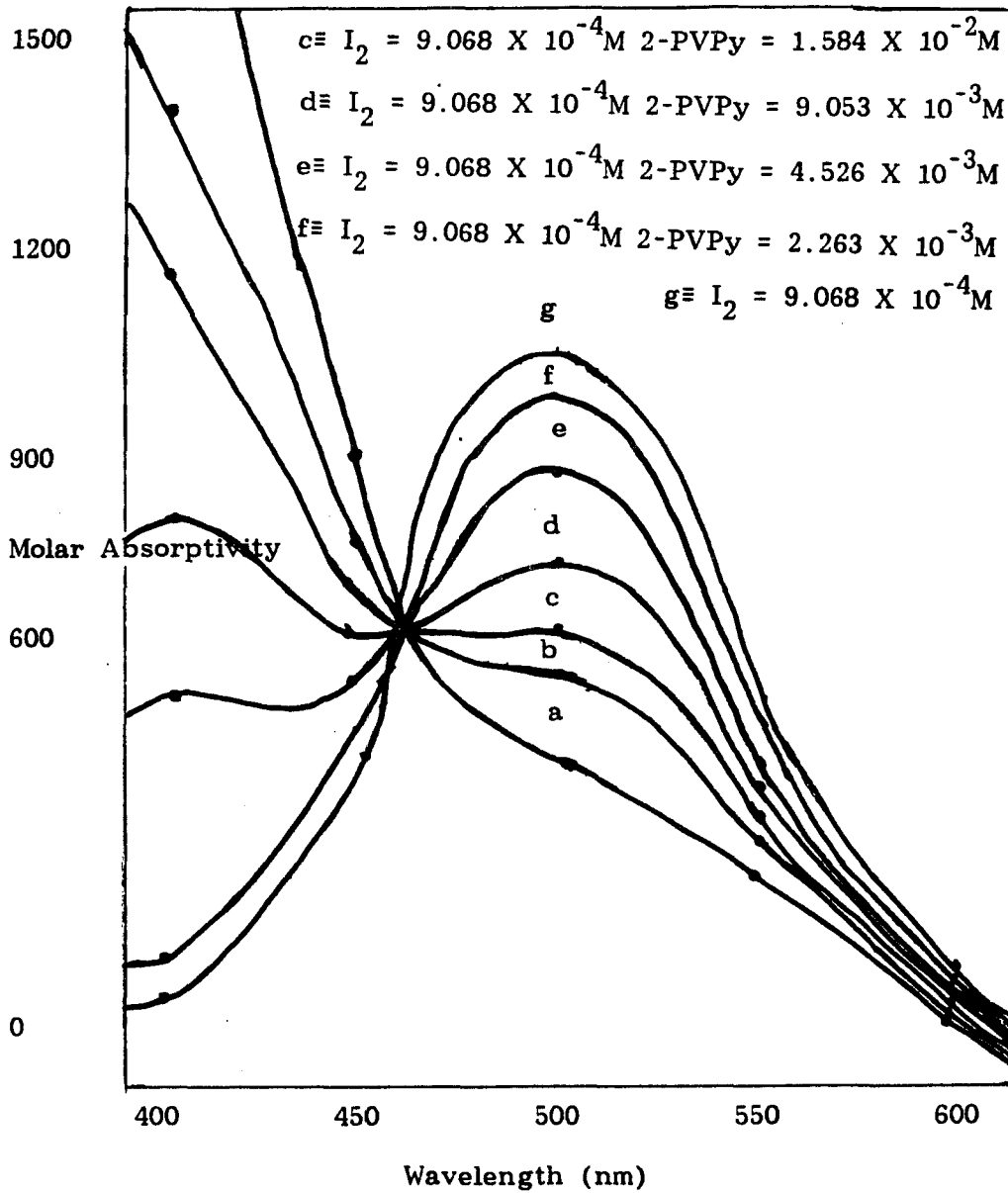


Figure 7: Visible spectra of $9.068 \times 10^{-4} \text{ M}$ iodine with various concentrations of 2-polyvinylpyridine in benzene

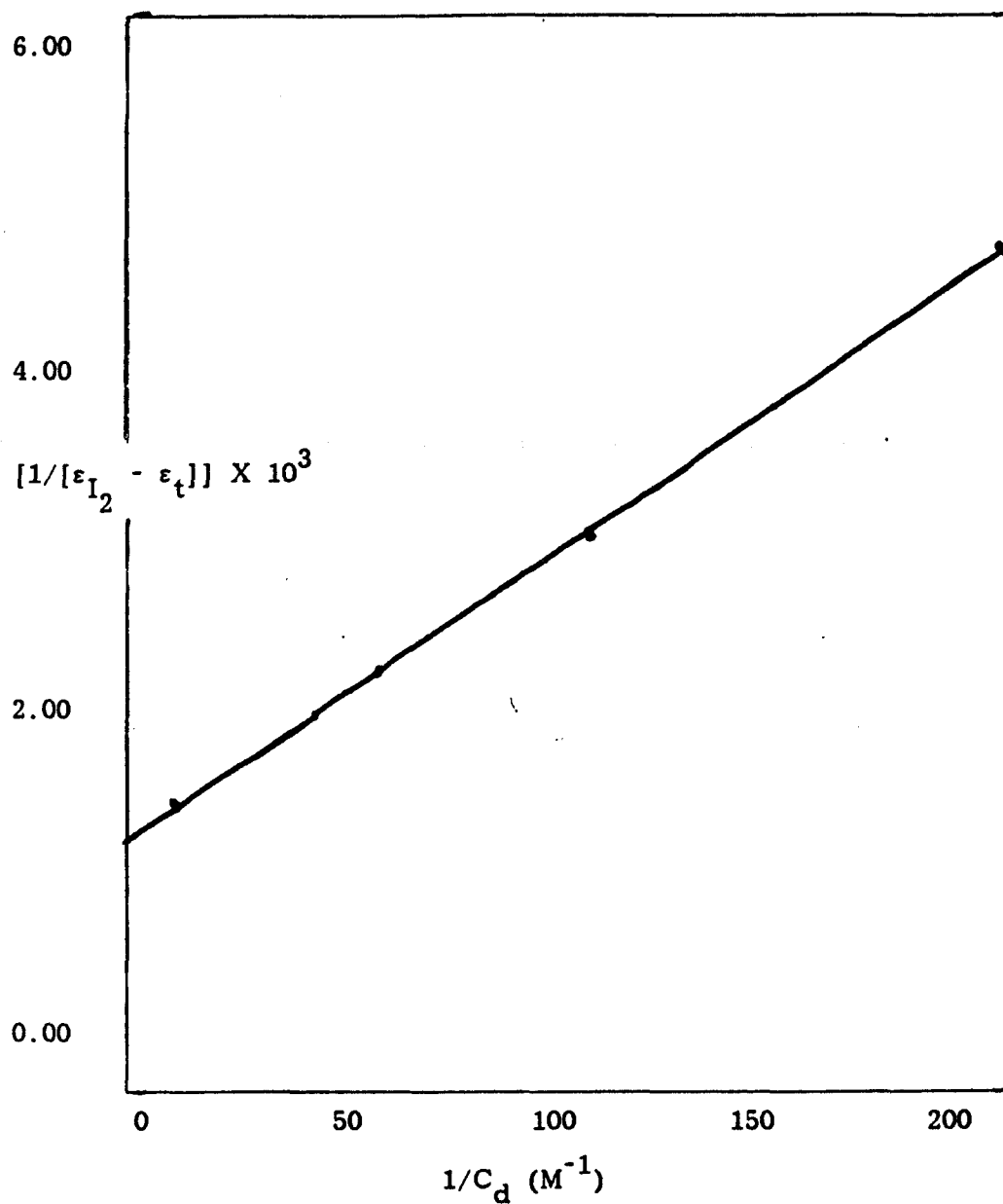


Figure 8: $[1/[\epsilon_{I_2} - \epsilon_t]] \times 10^3$ vs $1/C_d$ for 9.068×10^{-4} M I_2 with various 2-PVPy concentrations in benzene

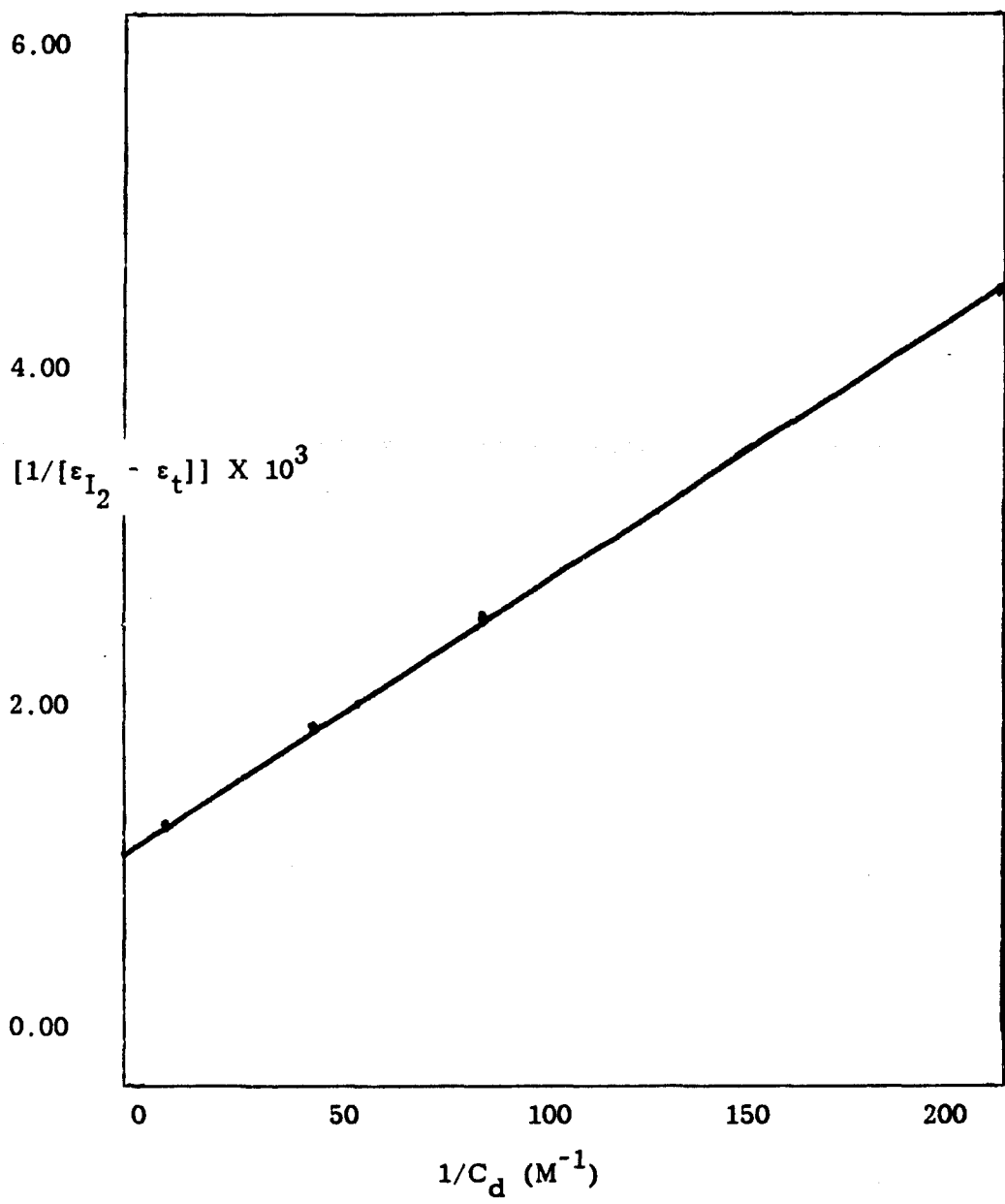


Figure 9: $[1/[\epsilon_{I_2} - \epsilon_t]] \times 10^3$ vs $1/C_d$ for $9.133 \times 10^{-4} M I_2$ with various Py concentrations in benzene

TABLE 1

Equilibrium Constants of Formation

Solvent	2-PVPI ₂ K _{eq} ^a	PyI ₂ K _{eq} ^a	PyI ₂ K _{eq} ^b
benzene ^c	72.2	72.6	82.9
1,2 dichloroethane	119	233	189
orthodichlorobenzene	155	318	367

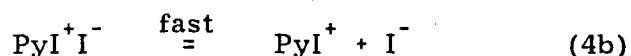
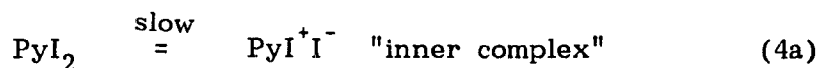
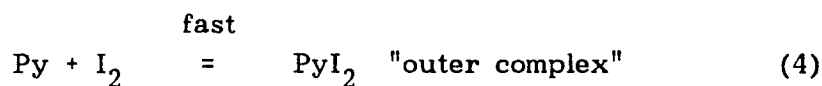
^aExperimental values

^bLiterature reported values

^cValues of K_{eq} in benzene have not been corrected for benzene-iodine complex formation.

3.1.2 Electrochemical Measurements in Solution

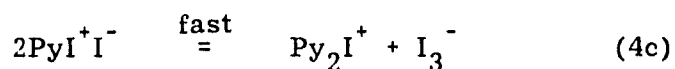
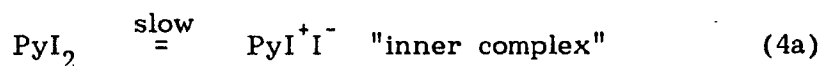
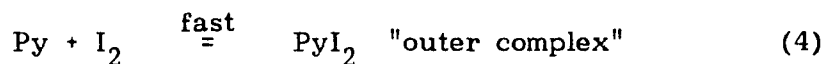
Mulliken²⁰ suggests that when iodine is dissolved in pyridine, the primary reactions to be considered are



where the "outer complex" is a molecular complex and the "inner complex" is essentially an ion pair. The third step illustrates dissociation of the ion pair assisted by a polar medium, in this case pyridine.

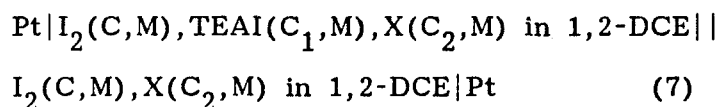
In considering the possible modes of interaction of pyridine with iodine, Mulliken believes that the energy of interaction in passing from "outer complex" to "inner complex" must overcome an energy barrier of considerable height. This would explain the slow increase with time of the electrical conductivity of Py-I₂ solutions.

We suggest the following set of reactions for 2-PVPy-I₂ and Py-I₂ in 1,2 dichloroethane, a modified version of the Mulliken formulation.



We will assume that the equilibrium of Reaction 4a lies far to the right. This simplifies our calculations and seems reasonable based on the consistency and reproducibility of our data. In Reaction 4c we have postulated formation of I_3^- rather than I^- , since at moderate to high concentrations of iodine, this is what is expected.^{1,2,6,7}

In our treatment of data from electrochemical cells of the type



where

X = 2-polyvinylpyridine or pyridine

TEAI = tetraethylammonium iodide

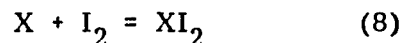
1,2-DCE = 1,2 dichloroethane

C = nominal concentration of elemental iodine in 1,2-DCE

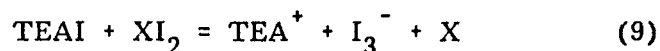
C_1 = nominal concentration of added TEAI

C_2 = nominal concentration of X in 1,2-DCE

We assume that all the I_2 is in its complexed form; that is the reaction

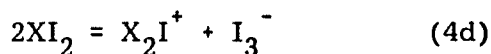


goes to completion. The equilibrium constants at room temperature for Equation 8 are in the range of 1.2×10^2 L/mole and 2.3×10^2 L/mole for 2-PVPy- I_2 and Py- I_2 in 1,2-DCE respectively. We also assume that the reaction



goes to completion. On the basis of the equilibrium constants of formation of the complexes and information in the literature on the equilibrium constant for Reaction 9^{11,12}, both of these assumptions appear reasonable. TEAI is used rather than sodium or potassium iodide because of its higher solubility and dissociation in 1,2-DCE.

We have obtained information on the equilibrium reaction in 1,2-DCE



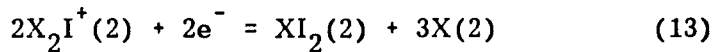
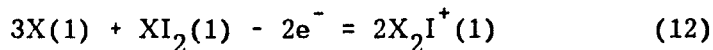
where the equilibrium constant may be expressed

$$K_{eq} = [a_{X_2I^+}] [a_{I_3^-}] / [a_{XI_2}]^2 \quad (10)$$

If the concentration of XI_2 is kept approximately constant, then

$$K' = K_{eq} [a_{XI_2}]^2 = [a_{X_2I^+}] [a_{I_3^-}] \quad (11)$$

Virtual electrochemical half-cell reactions for cells of the type described by Line Diagram 7 may be written



where half-cell 1 has TEAI(C_1) and half-cell 2 contains no TEAI. The concentrations of I_2 , as well as X , are assumed to be the same in both half-cells. The expression for the EMF, in volts, of such a cell at 25.0°C may be written

$$EMF = -.05916 \log [a_{X_2I^+(1)} / a_{X_2I^+(2)}] \quad (14)$$

We designate the equilibrium activity of X_2I^+ by the symbol X when no TEAI is present and by the symbol Y when TEAI is

present. The nominal concentration of TEAI is C_1 and may be substituted for activity in the equilibrium expression. Assuming the dissociation in Reaction 4d to be small

$$K' = Y(Y + C_1) = X^2 \quad (15)$$

X, Y and K' may be solved for by utilizing Equations 14 and 15.

Measurements were made on fresh and stored solutions at 25.0°C with electrochemical cells of the type described by Line Diagram 7, with the same nominal concentration of I_2 and X in both half-cells and TEAI present in one half-cell. Measurements were performed using the two compartment "H" type cell. A three compartment cell using .2M tetraethylammonium picrate as a salt bridge in the middle compartment showed no difference in measured EMF values and less convenience when compared to the "H" type cell.

In the cells containing Py- I_2 in 1,2-DCE, the pyridine concentration ranged from $2.483 \times 10^{-2}M$ to $2.972 \times 10^{-1}M$, and the iodine concentration ranged from $2.558 \times 10^{-4}M$ to $2.980 \times 10^{-3}M$. For the 2-PVPy- I_2 in 1,2-DCE cells, the 2-PVPy concentration ranged from $2.536 \times 10^{-2}M$ to $2.979 \times 10^{-1}M$ and the iodine concentration ranged from $2.708 \times 10^{-4}M$ to $2.963 \times 10^{-3}M$.

Upon investigation, it was found that the apparent percent ionization first increased with time and then leveled off after about

seven days for the Py-I_2 and 2-PVPy-I_2 systems. This behavior can be seen in Figure 10. Based on these measurements all results reported are for solutions stored ten days or more. Similar results have been obtained for PyI_2 in pure pyridine, where the apparent percent ionization is found to increase rapidly in the first few days and then levels off in approximately one week¹³.

Useful measurements could be made on solutions stored for up to one month. Unstable voltages were observed for cells prepared from solutions stored more than one month. One cause may be the dehydrochlorination of 1,2-DCE by pyridine and pyridine related compounds¹⁴.

Typical data obtained on a cell using 2-PVPy-I_2 in 1,2-DCE and a cell using Py-I_2 in 1,2-DCE are presented in Tables 2 and 3 and Figures 11 and 12 respectively. The nominal concentration of iodine in both cells was approximately $2 \times 10^{-3}\text{M}$. The nominal concentrations of pyridine and 2-polyvinylpyridine were approximately $2 \times 10^{-1}\text{M}$. Additions of TEAI to one half-cell gave TEAI nominal concentrations between 1% and 10% of the nominal iodine concentration. The first addition to the 2-PVPy-I_2 cell gave a nominal concentration of TEAI of $2.23 \times 10^{-5}\text{M}$. The EMF, measured intermittently over a period of forty minutes had a steady value of $1.25 \pm .03\text{mV}$. The nominal concentration of TEAI was increased nine additional times and measurements of the EMF made.

Calculated values of K' and X deviate slightly from each other but may be considered constant within experimental error. All experimental data were reproducible and consistent.

The calculated activities of X_2I^+ and the percent ionization of iodine based on Reaction 4d are presented in Tables 4 and 5. The values of the average percent ionization, $24.1 \pm 2.0\%$ for PyI_2 and $23.4 \pm 1.8\%$ for 2-PV PyI_2 , are very close.

Values of the equilibrium constant for the ionization of XI_2 corresponding to Equation 10 and Reaction 4d were calculated from the data in Tables 4 and 5. The average values for PyI_2 and 2-PV PyI_2 were $.0254 \pm .005$ and $.0236 \pm .004$ respectively. The values for both the equilibrium constant and percent ionization are in excellent agreement with the values obtained for PyI_2 in pure pyridine¹³.

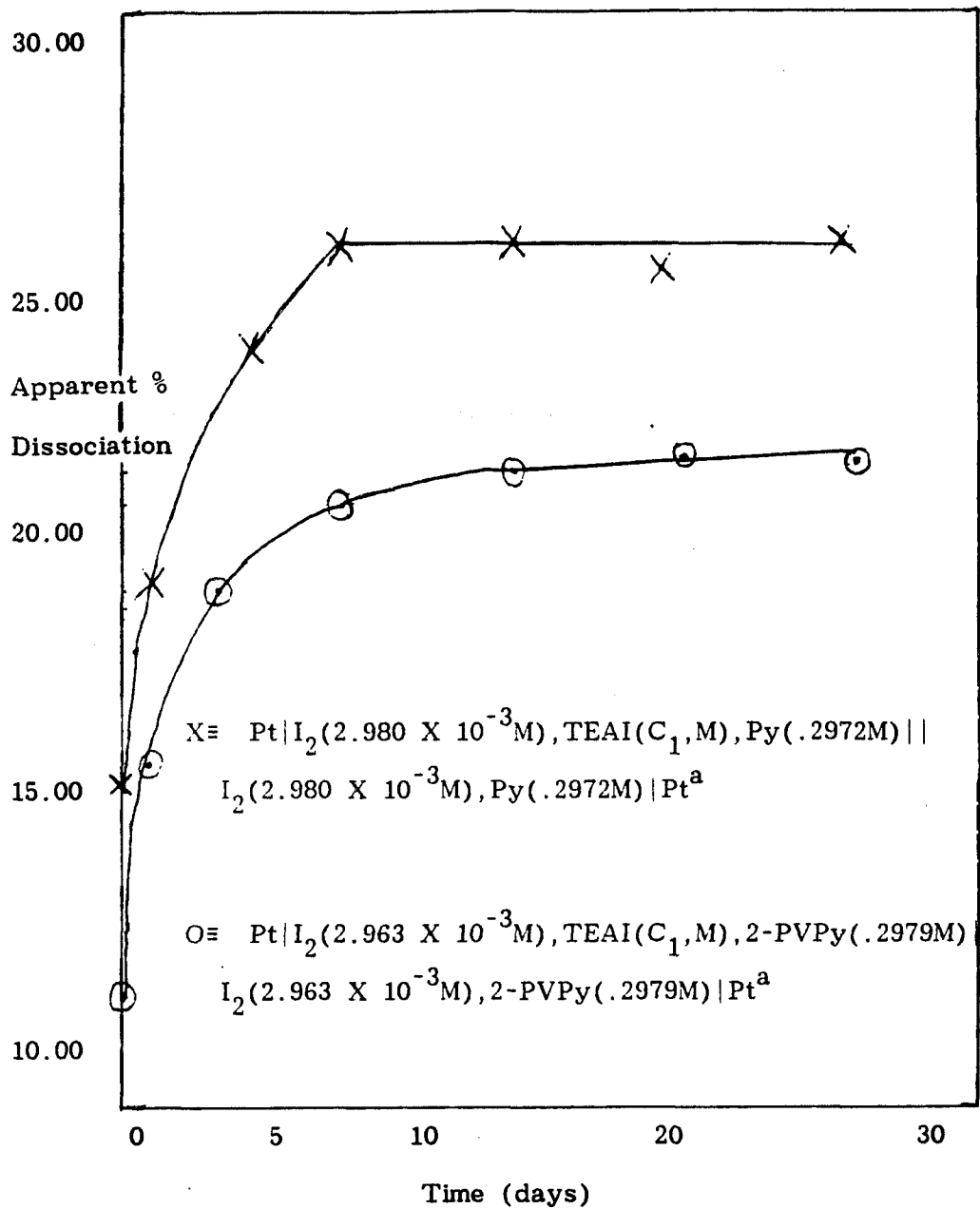
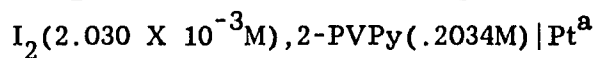
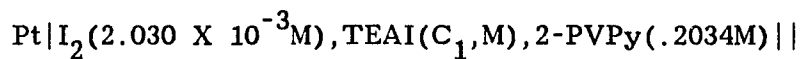


Figure 10: Variation of the apparent percent ionization of 2-PVPyI₂ and PyI₂ with time in 1,2 dichloroethane

TABLE 2

EMF data on the cell

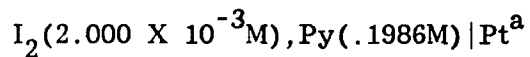
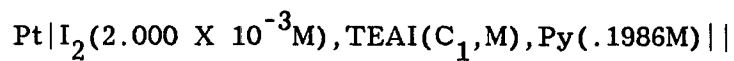


C_1 MX10 ⁵	EMF mV	Y MX10 ⁴	K' M ² X10 ⁸	X MX10 ⁴
2.23	1.25	2.18	5.24	2.29
4.37	2.49	2.04	5.07	2.25
6.43	3.72	1.92	4.90	2.21
8.42	4.91	1.81	4.79	2.19
10.3	6.03	1.72	4.76	2.18
12.2	7.05	1.66	4.80	2.19
14.0	8.04	1.60	4.81	2.19
15.7	9.00	1.54	4.80	2.19
17.3	9.95	1.48	4.76	2.18
18.9	10.93	1.41	4.67	2.16
				2.21 ± .028

^aOxidation occurs on the side of the cell containing TEAI.

TABLE 3

EMF data on the cell



C_1 MX10 ⁵	EMF mV	Y MX10 ⁴	K' M ² X10 ⁸	X MX10 ⁴
2.20	1.25	2.15	5.11	2.26
4.32	2.46	2.05	5.06	2.25
6.35	3.60	1.96	5.10	2.26
8.31	4.67	1.90	5.17	2.27
10.2	5.85	1.77	4.93	2.22
12.0	6.94	1.68	4.83	2.20
13.8	8.01	1.59	4.73	2.18
15.5	9.07	1.51	4.61	2.15
17.1	10.09	1.44	4.51	2.13
18.7	11.08	1.37	4.42	2.10
				2.20 ± .043

^aOxidation occurs on the side of the cell containing TEAI.

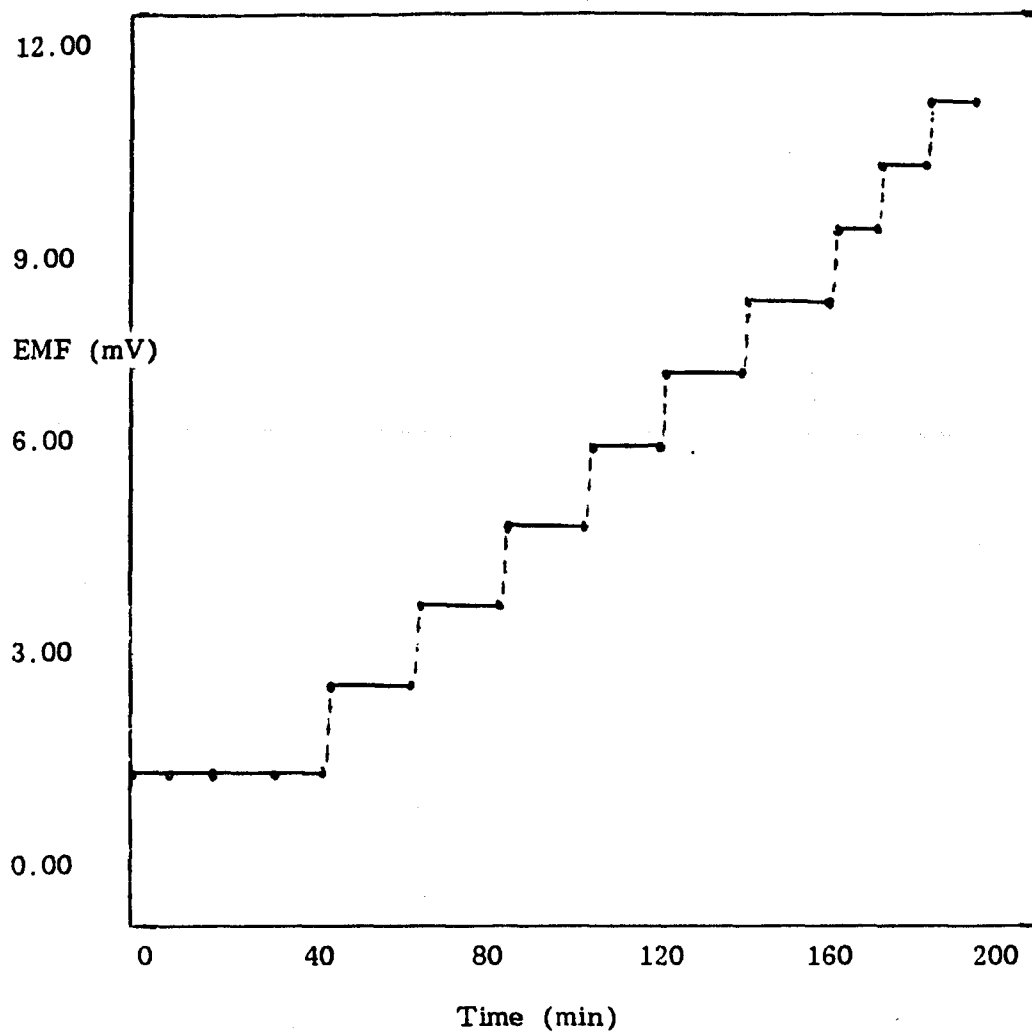


Figure 11: EMF data on the cell from Table 2. The vertical dashed lines refer to additions of TEAI

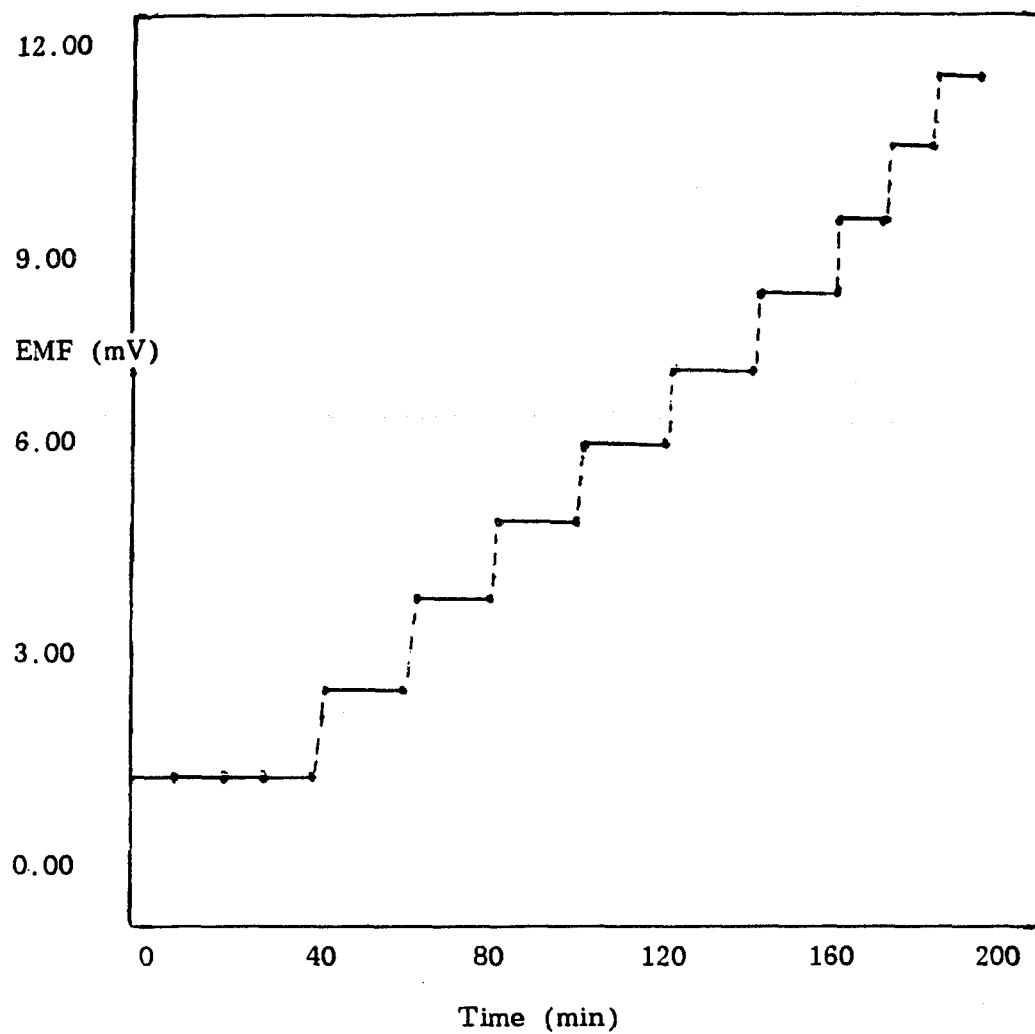


Figure 12: EMF data on the cell from Table 3. The vertical dashed lines refer to additions of TEAI

TABLE 4

Summary of data from electrochemical cells of the type
described by Line Diagram 7

2-PVPy Nominal Concn MX10 ²	I ₂ Nominal Concn MX10 ⁴	I ⁺ Activity MX10 ⁴	I ₂ ^a Ionization %	Equn 4d ^a K _{eq} M ² X10 ²
2.536	2.708	.344± .013	25.4	2.90
4.968	5.165	.607± .087	25.1	2.36
10.00	11.12	1.39± .087	25.1	2.78
20.34	20.30	2.21± .028	21.8	1.94
29.79	29.63	3.16± .034	21.3	1.84
			23.4±1.7	2.36±.48

^aAverage values taken after solutions are stored for two weeks.

TABLE 5

Summary of data from electrochemical cells of the type
described by Line Diagram 7

Py	I ₂	I ⁺	I ₂ ^a	Equn 4d ^a
Nominal	Nominal	Activity	Ionization	K _{eq}
Concn	Concn	MX10 ⁴	%	M ² X10 ²
MX10 ²	MX10 ⁴			
2.483	2.558	.340± .010	26.6	3.28
4.965	4.920	.546± .003	22.2	2.03
9.031	10.12	1.21± .033	24.0	2.47
19.86	20.00	2.20± .043	22.0	1.99
29.72	29.80	3.80± .075	25.5	2.93
			24.1±1.6	2.54±.56

^aAverage values taken after solutions are stored for two weeks

3.1.3 Ultraviolet-Visible Spectroscopy

We have utilized uv-visible spectroscopy to examine differences between fresh and stored solutions of Py-I₂ in 1,2-DCE and 2-PVPy-I₂ in 1,2-DCE.

In Figure 13 data are presented on solutions of $4.986 \times 10^{-2} \text{M}$ 2-PVPy and $5.165 \times 10^{-4} \text{M}$ I₂ in 1,2-DCE and $4.965 \times 10^{-2} \text{M}$ Py and $4.920 \times 10^{-4} \text{M}$ I₂ in 1,2-DCE, where the variation of molar absorptivity with time is monitored. Molar absorptivity is defined as the absorbance per centimeter per molar concentration of iodine.

The absorption peaks of the complexes at 365nm-367nm reached a maximum intensity after ten days, and then were essentially constant over a period of two to three weeks. This result is in agreement with our ionization data obtained from the electrochemical cell measurements. This maximum, as well as the maximum at 300nm are known to be due to triiodide ion¹⁸. The maximum at 300nm does not show a clear trend possibly due to other species present which may also absorb in this region. ϵ_{max} for the peaks at 376nm are 16,000 and 10,000 for 2-PVPy-I₂ and Py-I₂ respectively. The reason for the difference in molar absorptivity between Py-I₂ and 2-PVPy-I₂ presented in Figure 13 is unknown at this time. This data agrees well with data on Py-I₂ in pure pyridine at high iodine concentrations where a maximum at 367nm with $\epsilon_{\text{max}}=16,000$ is found for solutions stored at least six days¹³. If we

compare our data to the data obtained in pure pyridine with a similar iodine concentration, we see a great difference in the systems. For iodine concentrations of 10^{-4} M to 10^{-2} M in pure pyridine a uv-vis absorption is found at 367nm and 300nm in fresh solutions. Over a period of about one week the peak at 367nm moves to 422nm. The peak at 422nm is attributed to the unionized PyI_2 molecular complex¹³. In our solvent systems for Py and 2-PVPy we do not observe the presence of the species that gives rise to the absorption at 422nm in pure pyridine.

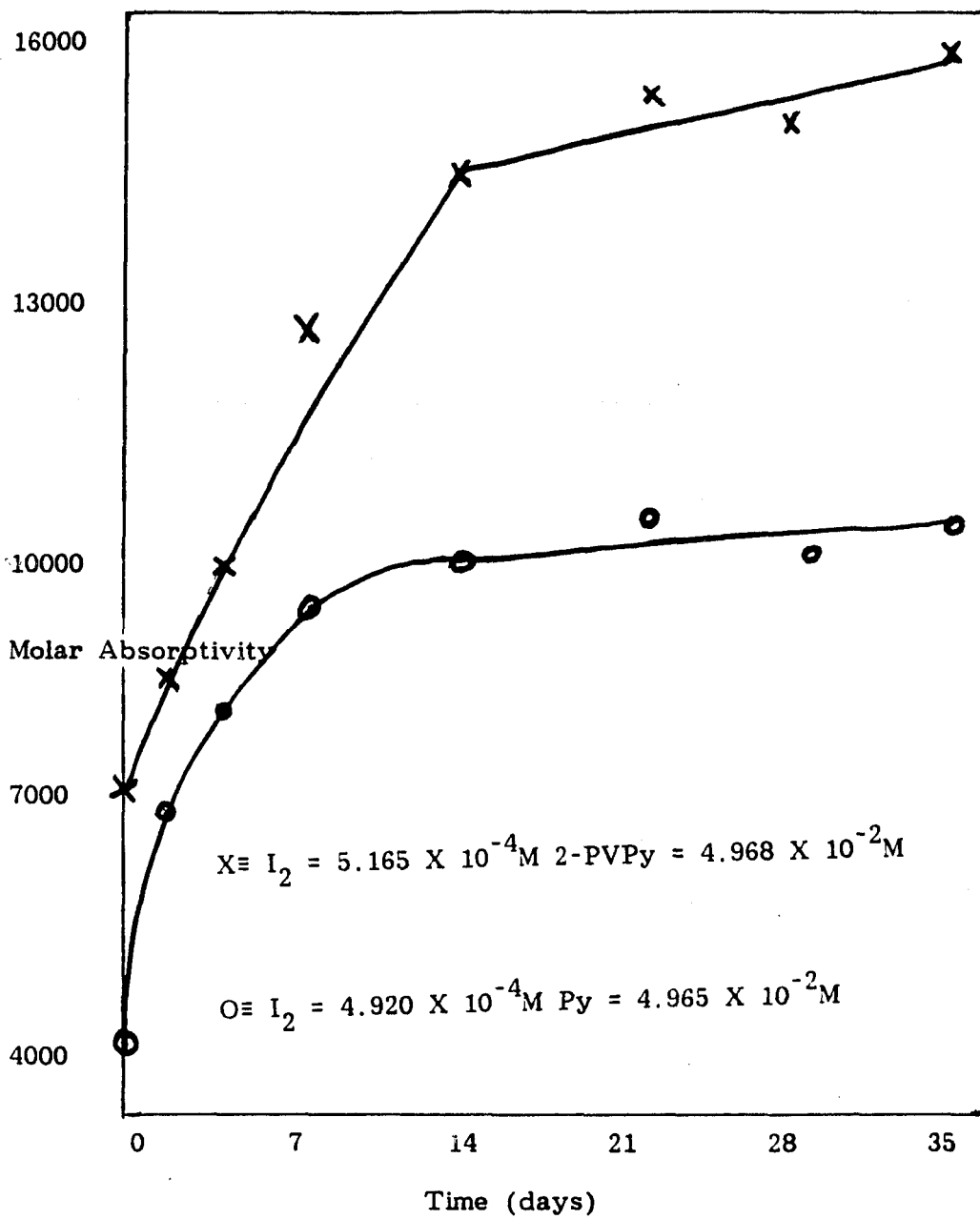


Figure 13: Variation of molar absorptivity of Py-I₂ and 2-PVPy-I₂ at 365nm with time

3.1.4 Conductivity Measurements

Measurements of conductivity were made on Py-I_2 in 1,2-DCE and 2-PVPy- I_2 in 1,2-DCE. These are the same solutions for which the electrochemical cell measurements were made. The variation of specific conductivity with time for these solutions are summarized in Tables 6 and 7 and in Figures 14 and 15. The conductivity is observed to increase with increasing concentration and time as we would expect from the electrochemical cell data. The conductivity levels off in seven to ten days as we would also predict from our previous data.

This result is in marked contrast to the results obtained on the conductivity of Py-I_2 in pure pyridine. In this system specific conductivity does not level off but continues to grow with increasing time after seven days¹³. Changing solvents from pyridine to 1,2-DCE has apparently reduced any side reactions or degradation reactions that the continually rising conductivity of Py-I_2 in pyridine has been attributed to.

A prediction from our electrochemical cell data would be a linear dependence of conductivity of stored solutions on iodine concentration. Figure 16 shows this to be an accurate expectation. These data differ from Py-I_2 in pure pyridine where the relationship between conductivity and iodine concentration is nonlinear¹³.

TABLE 6

Summary of data from conductivity cells of 2-PVPy-I₂

2-PVPy Nominal Concn MX10 ²	I ₂ Nominal Concn MX10 ⁴	$\sigma_0 \times 10^5$ (ohm cm) ⁻¹	$\sigma_1 \times 10^5$ (ohm cm) ⁻¹	$\sigma_2 \times 10^5$ (ohm cm) ⁻¹
2.536	2.708	.307	.558	.562
4.968	5.165	.436	.937	.934
10.00	11.12	.745	1.82	1.93
20.34	20.30	1.87	3.24	3.23
29.79	29.63	1.69	4.22	4.27

 σ_0 = specific conductivity of fresh solutions σ_1 = specific conductivity after two weeks σ_2 = specific conductivity after four weeks

TABLE 7

Summary of data from conductivity cells of Py-I₂

Py Nominal Concn MX10 ²	I ₂ Nominal Concn MX10 ⁴	$\sigma_0 \times 10^5$ (ohm cm) ⁻¹	$\sigma_1 \times 10^5$ (ohm cm) ⁻¹	$\sigma_2 \times 10^5$ (ohm cm) ⁻¹
2.483	2.558	.236	.831	.845
4.965	4.920	.290	1.26	1.40
9.931	10.12	.226	2.07	2.02
19.86	20.00	.809	3.36	3.32
29.72	29.80	1.04	4.54	4.64

 σ_0 = specific conductivity of fresh solutions σ_1 = specific conductivity after two weeks σ_2 = specific conductivity after four weeks

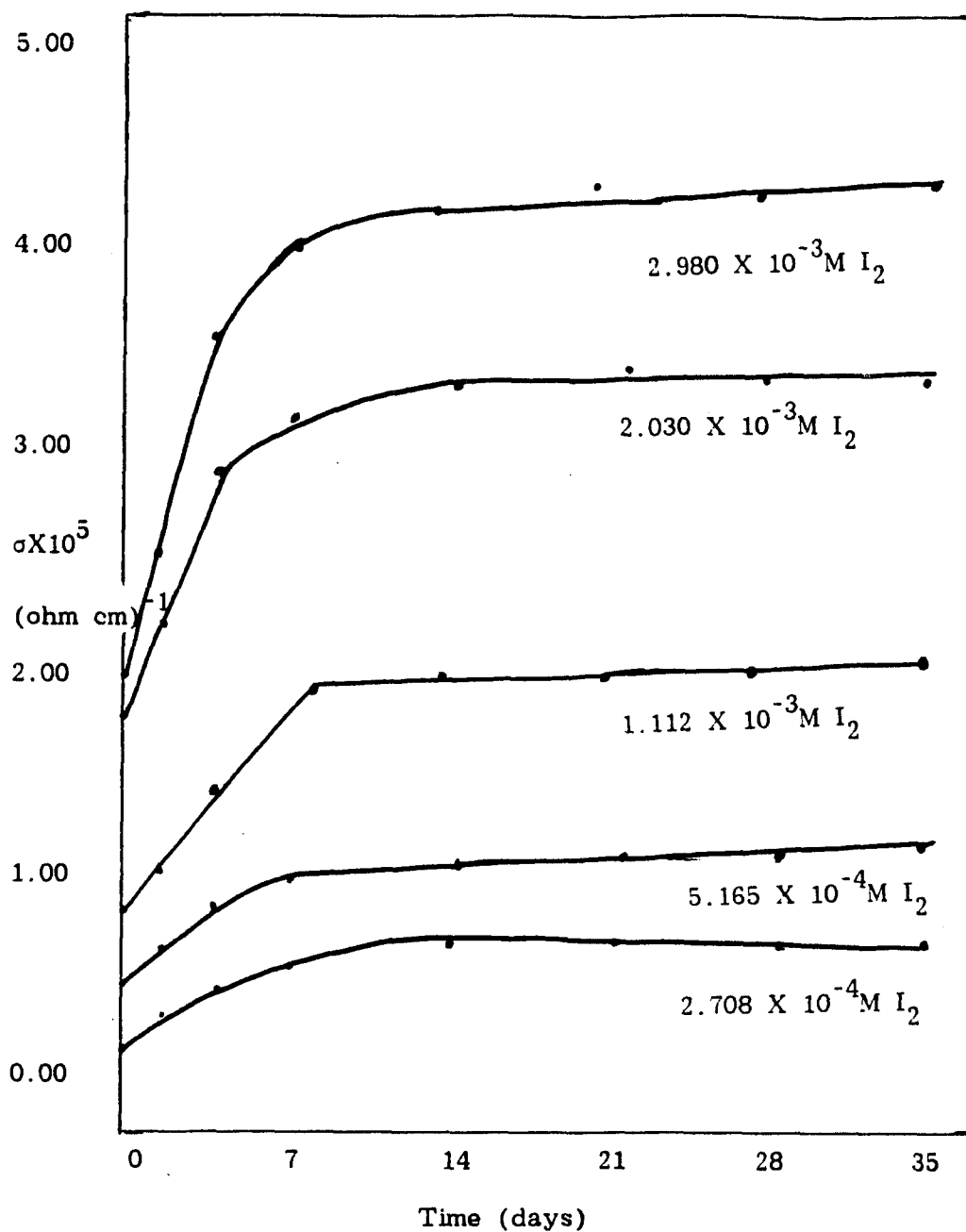


Figure 14: Variation of specific conductivity with iodine concentration and storage time for 2-PVPy- I_2 solutions

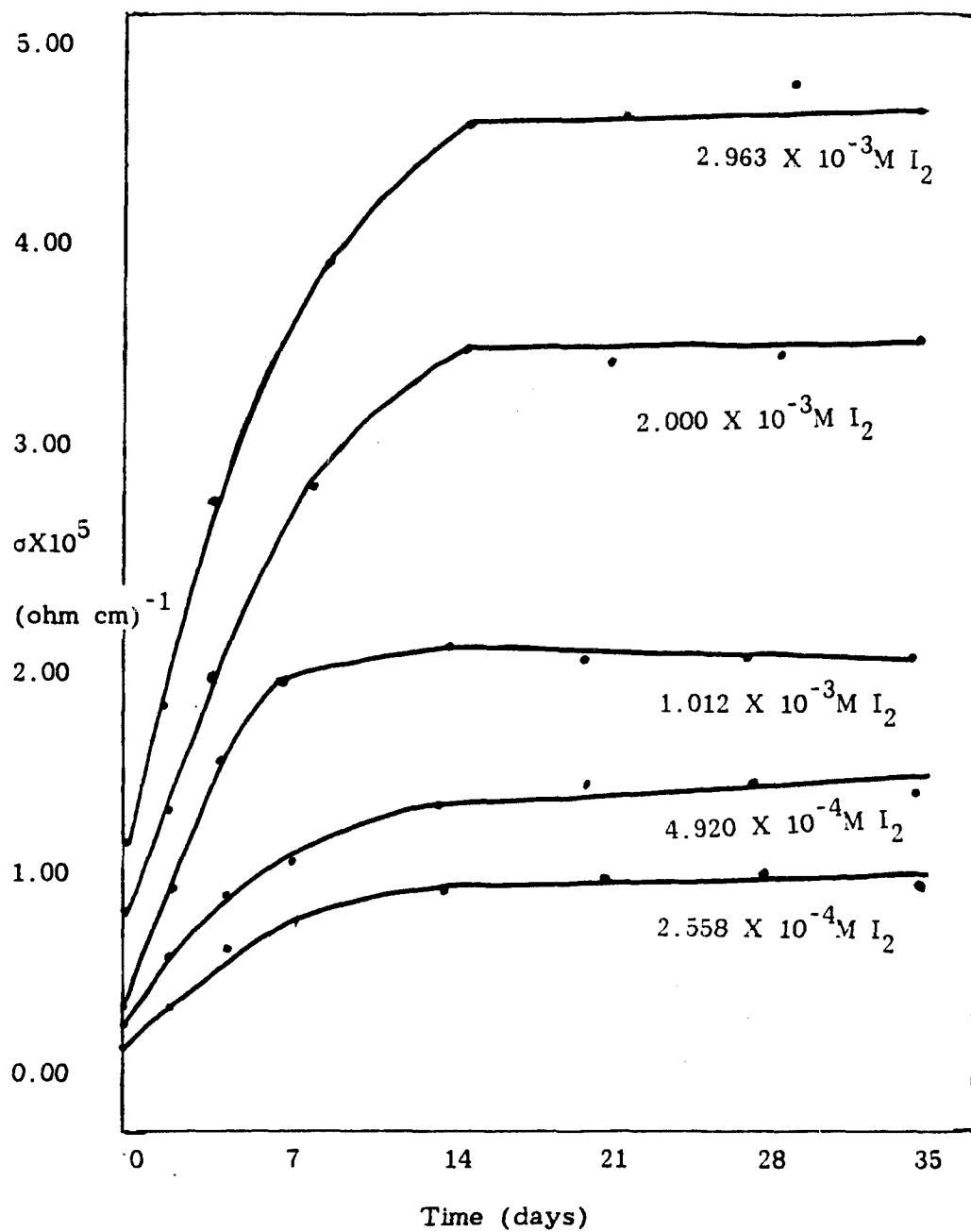


Figure 15: Variation of specific conductivity with iodine concentration and storage time for Py-I₂ solutions

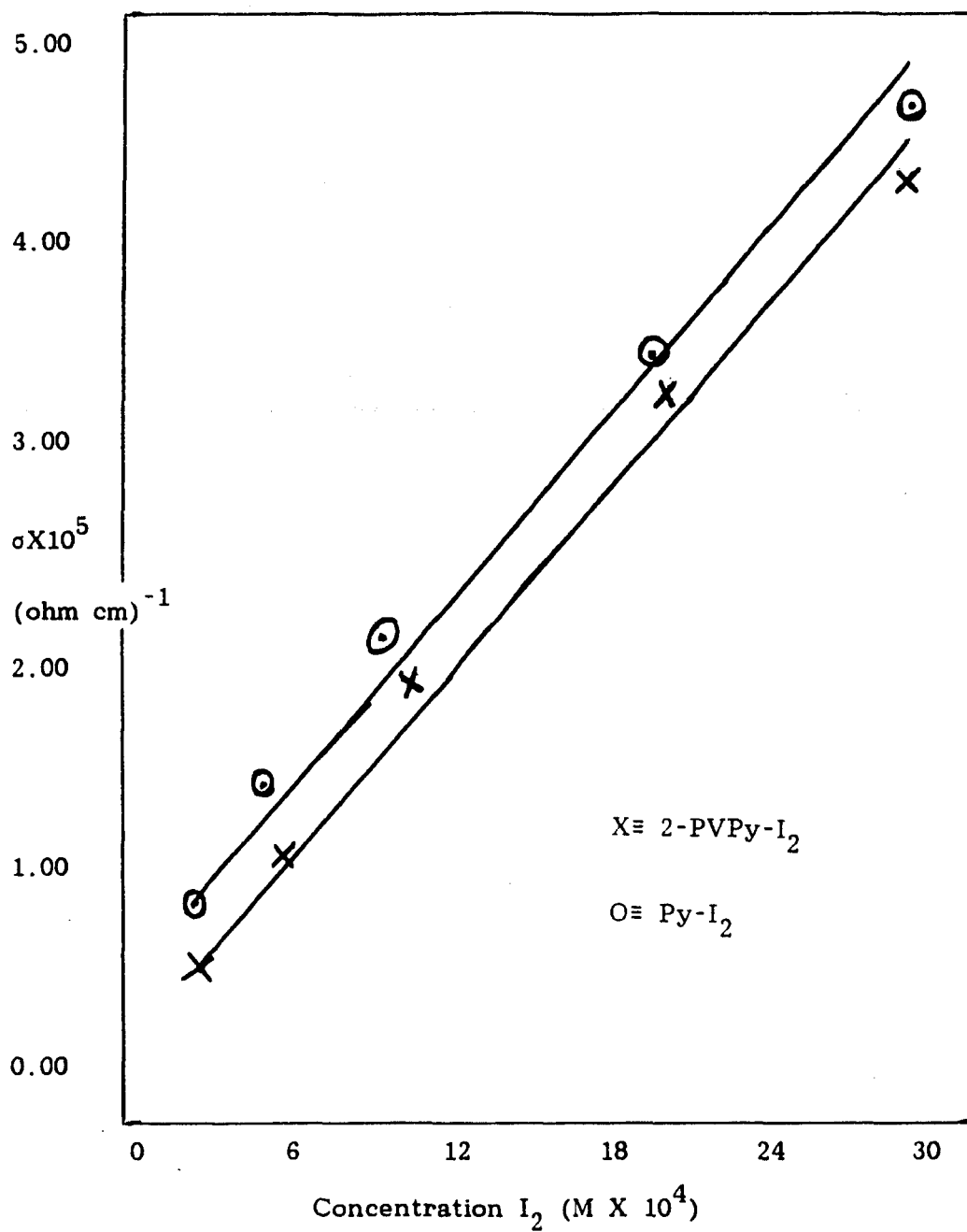
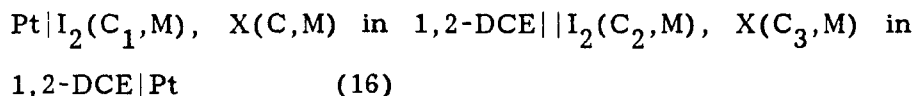


Figure 16: Variation of specific conductivity with concentration of I₂ for 2-PVPy-I₂ and Py-I₂ solutions stored four weeks

3.1.5 I₂ Concentration Cell Measurements

Concentration cell measurements were made at 25.0°C on electrochemical cells of the type



where

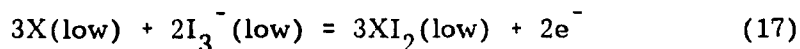
C₁ and C₂ = different nominal concentrations of I₂

X = Py or 2-PVPy

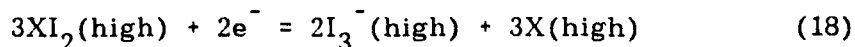
C and C₃ = nominal concentrations of X

Measurements were made using a two compartment "H" cell after the use of a three compartment cell with .15M tetraethylammonium picrate in the middle compartment showed no apparent improvement in the data.

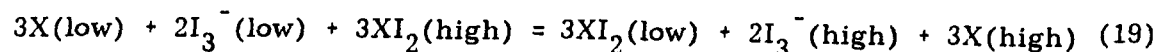
We may theoretically calculate values of the EMF expected for these types of concentration cells, using the assumption that the mechanism expressed in Reactions 12 and 13 are pertinent. For this mechanism, assuming that the complex formed is XI₂, we can write



and



where the oxidation half-reaction occurs on the side of the cell containing the lower I₂ concentration. The overall reaction may be written



The theoretical EMF at 25.0°C calculated using Reactions 19 and 8 is

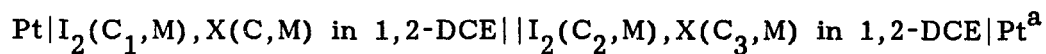
$$EMF_{\text{theo}} = [.05916/2] \log \left[\frac{[I_2(\text{high})]}{[I_2(\text{low})]} \left[\frac{[X(\text{low})]}{[X(\text{high})]} \right]^3 \right] \quad (20)$$

A comparison between theoretical values of the EMF and experimental values of the EMF for some selected solutions are presented in Tables 8 and 9. Experimental values are very unstable in fresh solutions, and in poor agreement with the theoretically predicted values. EMF values are very stable for cells made from solutions stored two weeks or more, but values still differ widely from the theoretical values. These discrepancies indicate that processes other than those discussed may be taking place in these solutions.

Cells of this type using pure pyridine as the solvent give experimental values which are much closer to the theoretically predicted values for high iodine concentrations¹³. For comparable I₂ concentrations, however, the experimental values in pure pyridine also differ widely from theoretically predicted values. The above results indicate the complexity of these systems.

TABLE 8

EMF data on cells of the type



Py	I ₂	Py	I ₂	EMF	EMF
Nominal	Nominal	Nominal	Nominal	Exp.	Theo
C	C ₁	C ₃	C ₂	mV	mV
M	MX10 ³	M	MX10 ³		
.2972	2.980	.2972	1.490	39.5 ^b	9.22
				46.2 ^c	
				32.1 ^d	
.2972	2.980	.2972	.745	83.2 ^b	18.23
				90.5 ^c	
				61.5 ^d	

^aOxidation occurs on the side of the cell with the lower iodine concentration.

^bFresh solutions

^cOne week old solutions

^dTwo week old solutions

TABLE 9

EMF data on cells of the type

$$\text{Pt}|\text{I}_2(\text{C}_1, \text{M}), \text{X}(\text{C}, \text{M}) \text{ in } 1, 2\text{-DCE} || \text{I}_2(\text{C}_2, \text{M}), \text{X}(\text{C}_3, \text{M}) \text{ in } 1, 2\text{-DCE}|\text{Pt}^{\text{a}}$$

2-PVPy Nominal C M	I ₂ Nominal C ₁ MX10 ³	2-PVPy Nominal C ₃ M	I ₂ Nominal C ₂ MX10 ³	EMF Exp. mV	EMF Theo mV
.2979	2.963	2.979	1.482	21.7 ^b 47.9 ^c 30.4 ^d	9.10
.2979	2.963	2.979	.741	44.8 ^b 79.5 ^c 53.3 ^d	18.10

^aOxidation occurs on the side of the cell with the lower iodine concentration.

^bFresh solutions

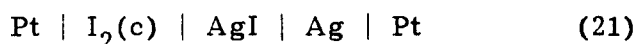
^cOne week old solutions

^dTwo week old solutions

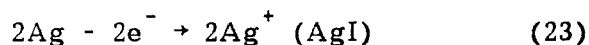
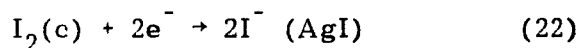
3.2 2-POLYVINYLPIRIDINE-IODINE AND OTHER SOLID-STATE COMPLEXES

3.2.1 Electrochemical Measurements

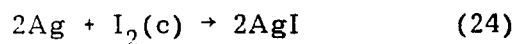
EMF data were obtained at 25.0°C on solid-state electrochemical cells of the type



$\text{I}_2(\text{c})$ represents pure iodine or iodine complexed in varying amounts with several polycyclic compounds, Perylene (Pe), Pyrene (Pyr), 2-PVPy, and the two types of pyrolyzed polyacrylonitrile. We assume that the electrode reactions are



The overall reaction is



We also assume that all of these reactions are reversible. It follows from standard thermodynamic relationships that

$$\Delta G_{\text{I}_2} = \bar{G}_{\text{I}_2}(\text{c}) - \bar{G}_{\text{I}_2}^* = -nF[\varepsilon^* - \varepsilon] = RT \ln [a_{\text{I}_2} / a_{\text{I}_2}^*] \quad (25)$$

where

ΔG_{I_2} = the relative partial molar free energy of iodine; the difference between the partial molar free energy of complexed iodine and that of pure solid iodine

n = the number of electrons transferred

F = Faraday's constant

ε^* = EMF of the cell using pure solid iodine

ϵ = EMF of the cell using complexed iodine

$a_{I_2}^*$ = thermodynamic activity of pure iodine

a_{I_2} = thermodynamic activity of complexed iodine

EMF data obtained are shown in Figure 17. In Figure 17 data on PPAN-1- I_2 , and 2-PVPy- I_2 are compared to data on Pyr- I_2 and Pe- I_2 . Note that the breaks in the curves for PPAN-1- I_2 , PPAN-2- I_2 and 2-PVPy- I_2 occur at approximate compositions PPAN-1-(I_2)_{1.0}, PPAN-2-(I_2)_{1.0} and 2-PVPy-(I_2)_{2.3}. These compositions correspond to the maximum uptake of iodine from the vapor. We may conclude that the thermodynamic activity of iodine at and above these compositions approaches that of pure, solid iodine.

Free energies of formation of the complexes per mole of iodine, ΔG , were calculated by numerical integration of the expression¹⁵

$$\Delta G = \left[\frac{1 - X'_{I_2}}{X'_{I_2}} \right] \int_0^{X'_{I_2}} \left[\frac{\bar{G}_{I_2} - \bar{G}_{I_2}^*}{[1 - X_{I_2}]^2} \right] dX_{I_2} \quad (26)$$

where X_{I_2} is the mole fraction of complexed iodine and X'_{I_2} is the mole fraction of iodine at the composition where the thermodynamic activity of iodine approaches that of pure iodine. The data in Figure 17 were extrapolated to a mole ratio of iodine to organic substance of zero, since the integration of Equation 26 must start at $X_{I_2} = 0$.

X'_{I_2} values for PPAN-1- I_2 and 2-PVPy- I_2 were selected to correspond to iodine to organic substance mole ratios of 1.0 and 2.3 respectively. Since other studies¹⁶ have shown that the maximum uptake of iodine by pyrene is 2.0 mole ratio of iodine to pyrene, and maximum uptake of iodine by perylene is 2.9 mole ratio of iodine to perylene, these values were used for X'_{I_2} in these systems.

Free energies of formation of the complexes were calculated by applying Equation 26 to the data in Figure 17. The results are presented in Table 10. Literature values for the free energy of formation of $Pyr(I_2)_{2.0}$ and $Pe(I_2)_{2.9}$ calculated from vapor pressure measurements¹⁶ are given for comparison. Our values of the free energy of formation for AgI, $Pyr(I_2)_{2.0}$ and $Pe(I_2)_{2.9}$ are reasonably close to the values obtained using other methods. This supports the validity of the EMF method used here. The low magnitudes of the free energies of formation for all the complexes indicates that the bonding is weak between the iodine and the organic species.

EMF data obtained on PPAN- I_2 samples pyrolyzed by two different procedures are shown in Figure 18. The data on the two PPAN samples are very similar.

EMF data obtained of 2-PVPy- I_2 annealed at various temperatures is also presented in Figure 18. Increasing the annealing temperature results in a decreasing iodine activity. Samples

annealed at 150°C could not be measured for mole ratios of iodine to segmer greater than 1.8. The morphology of these samples made measurement impossible.

The EMF values for 2-PVPy-I₂ samples annealed at 50°C, 70°C, and 90°C approach that of pure iodine at a mole ratio of iodine to segmer of about 2.3. This data does not show correspondence to the phase diagram obtained by Phillips and Untereker¹⁷. This may be attributed to the complex nature of the phase diagram and the possibility that phase changes may not be completely reversible in this temperature range.

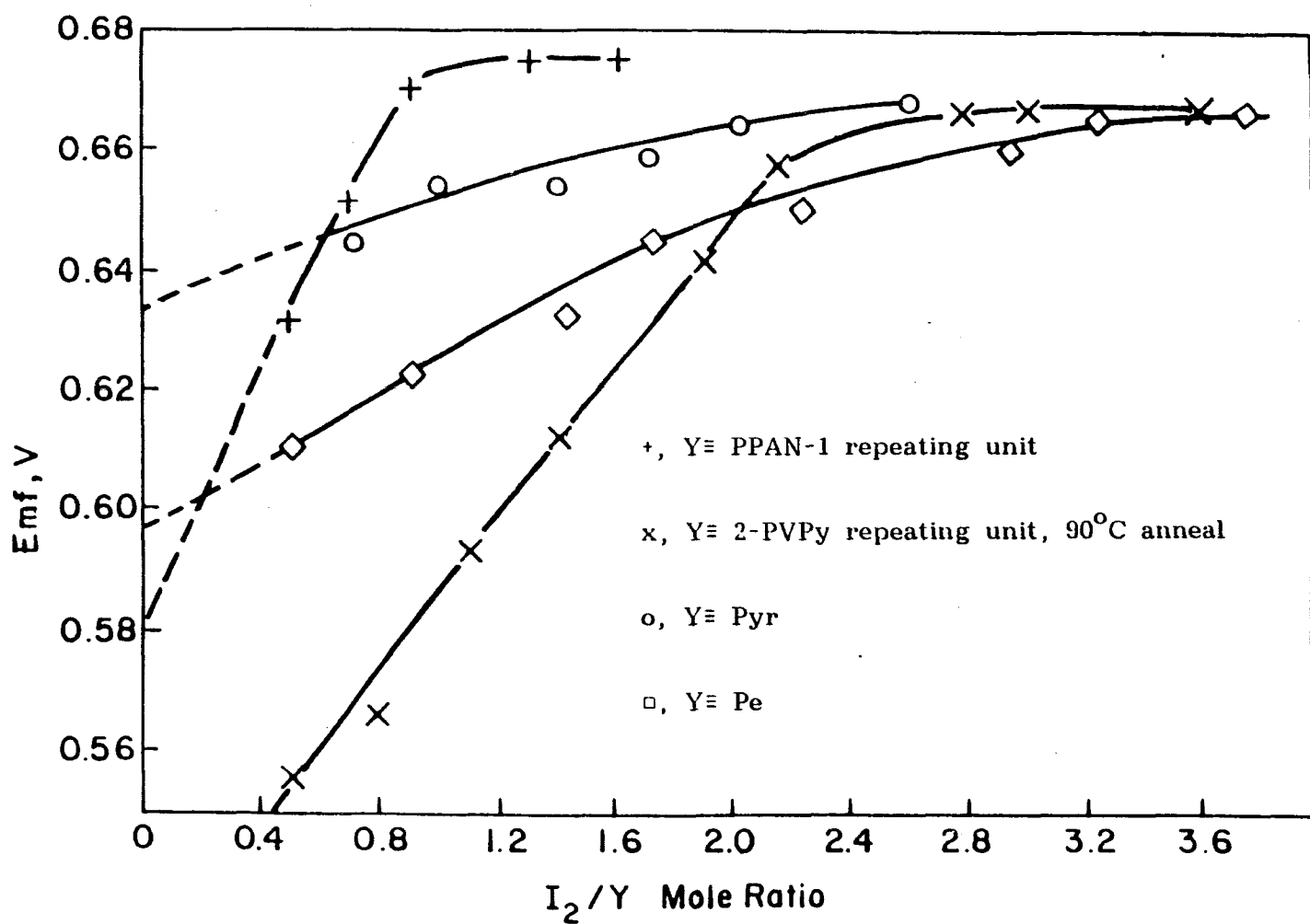


Figure 17: Variation of cell voltage with iodine content

TABLE 10

Comparison of free energies of formation of iodine complexes

Reaction	-ΔG	-ΔG
	EMF method ^a kcal/moleI ₂	Other methods kcal/moleI ₂
Ag + 0.5I ₂ → AgI	30.9	31.7 ^b
Pyr + 2I ₂ → Pyr(I ₂) _{2.0}	0.8	0.2 ^c
Pe + 2.9I ₂ → Pe(I ₂) _{2.9}	1.5	0.9 ^c
PPAN-1 + I ₂ → PPAN-1(I ₂) _{1.0}	2.0	
2-PVPy + 2.3I ₂ → 2-PVPy(I ₂) _{2.3}	3.2	

^aEstimated limits of error, ±1.0 kcal/moleI₂

^bHandbook of Chemistry and Physics, 1981, p. D-75

^cFrom reference 19, estimated limits of error, ±0.5 kcal/moleI₂

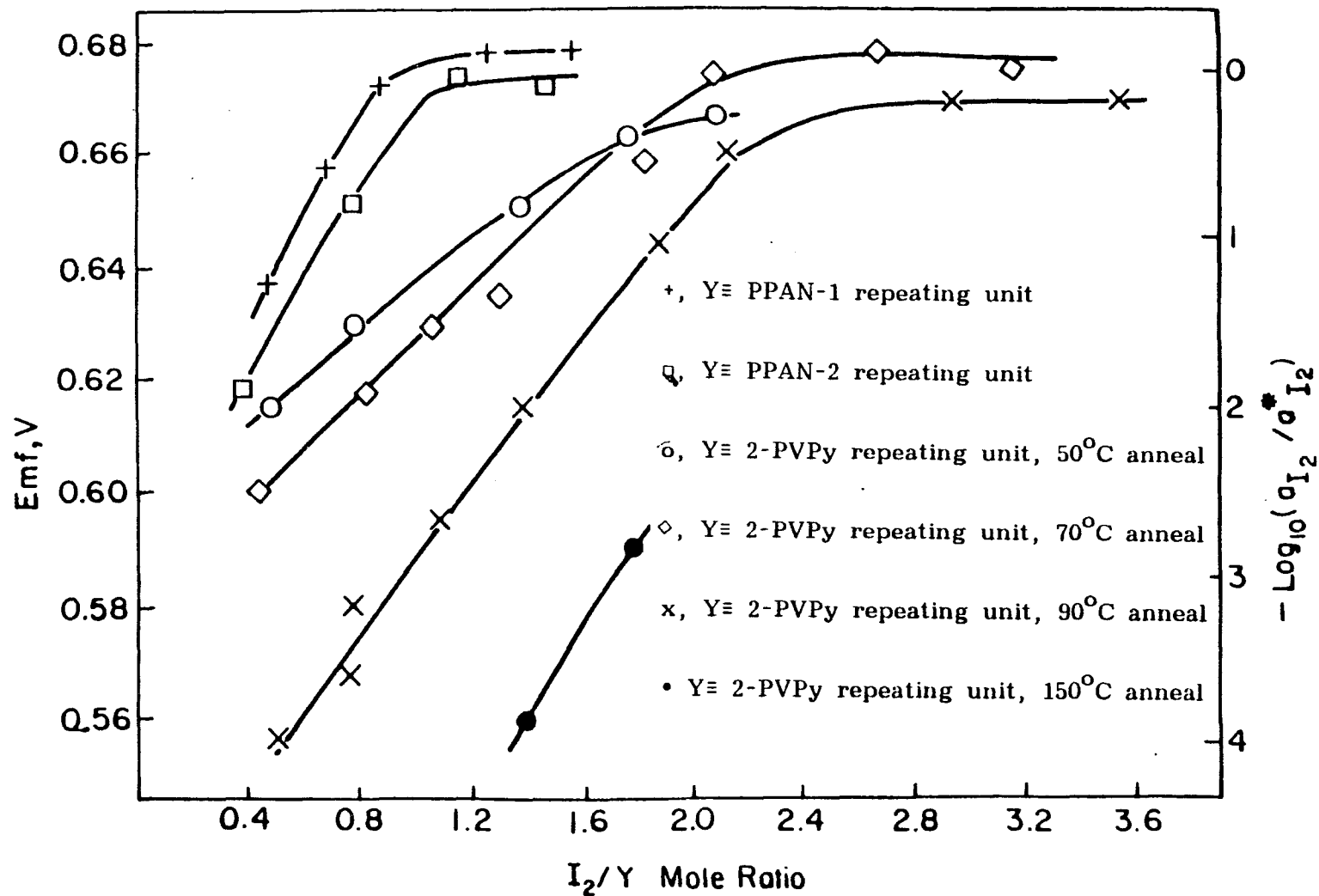


Figure 18: Variation of cell voltage with iodine content

3.2.2 Electrical Conductivity Measurements

Electrical conductivity measurements were made on PPAN-I₂ and 2-PVPy-I₂ samples at room temperature. The results are shown in Figures 19 and 20 respectively. It is observed that the PPAN-I₂ and 2-PVPy-I₂ curves reach plateaus at mole ratios of iodine to polymer of about 1.0 and 2.3 respectively. These ratios correspond to the compositions at which the thermodynamic activity of iodine approaches that of pure solid iodine. This implies that free iodine is present above a ratio of 1.0 for PPAN-I₂. The significance of the plateau is less clear for 2-PVPy-I₂ since the phase diagram is complex. Conductivity values reported in the literature for 2-PVPy-I₂ samples at mole ratios above 2.0¹⁷ are in the same range as our values. Electrical conductivity measured on PPAN-I₂ samples in the form of fibers rather than pressed pellets have been reported⁹. These values are somewhat higher than our values.

Figure 21 indicates that the method of preparation of the samples, direct addition of solid iodine to the polymers or addition of iodine through the vapor phase, does not influence the magnitude of the measured electrical conductivity.

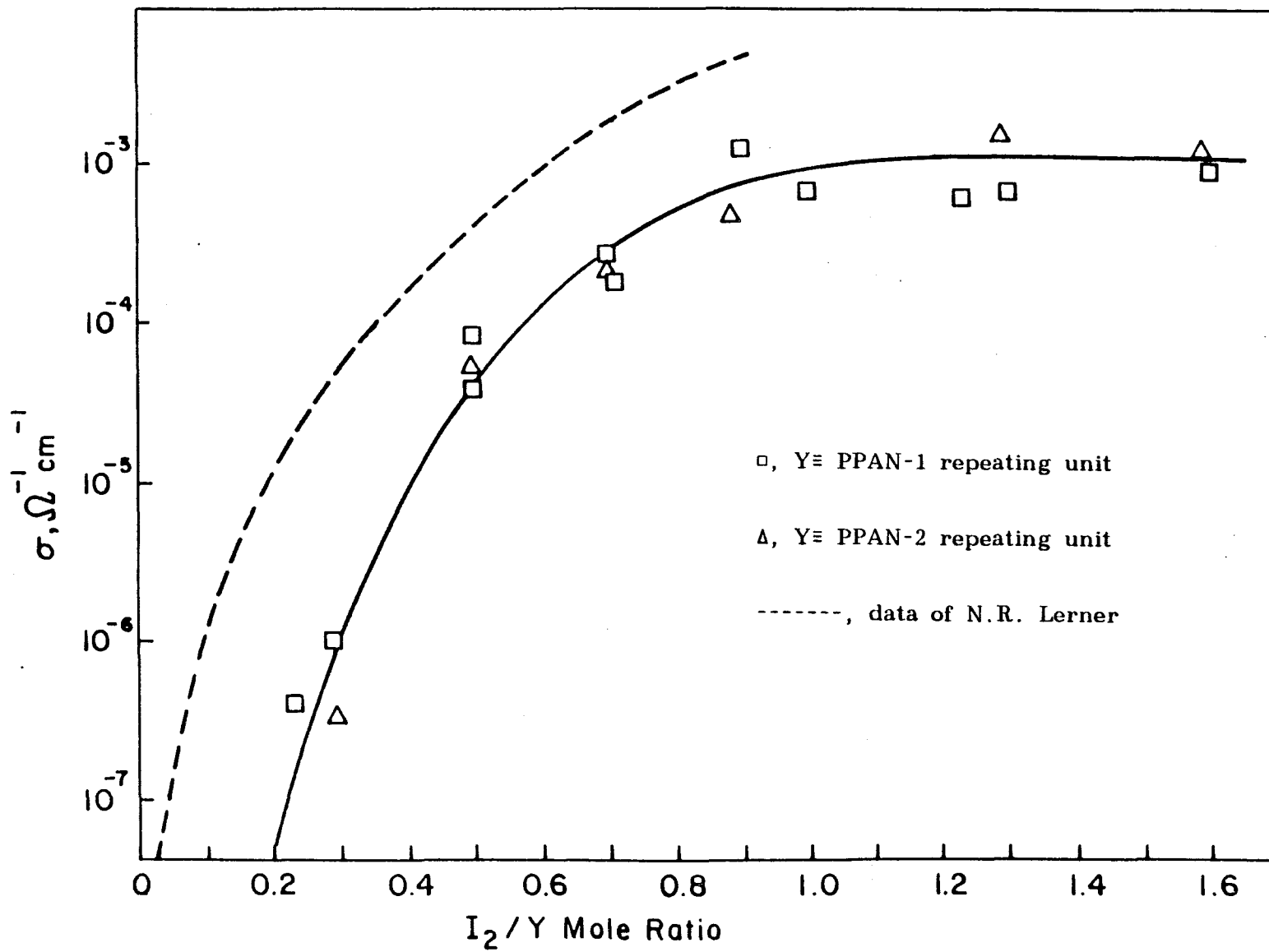


Figure 19: Variation of conductivity with iodine content

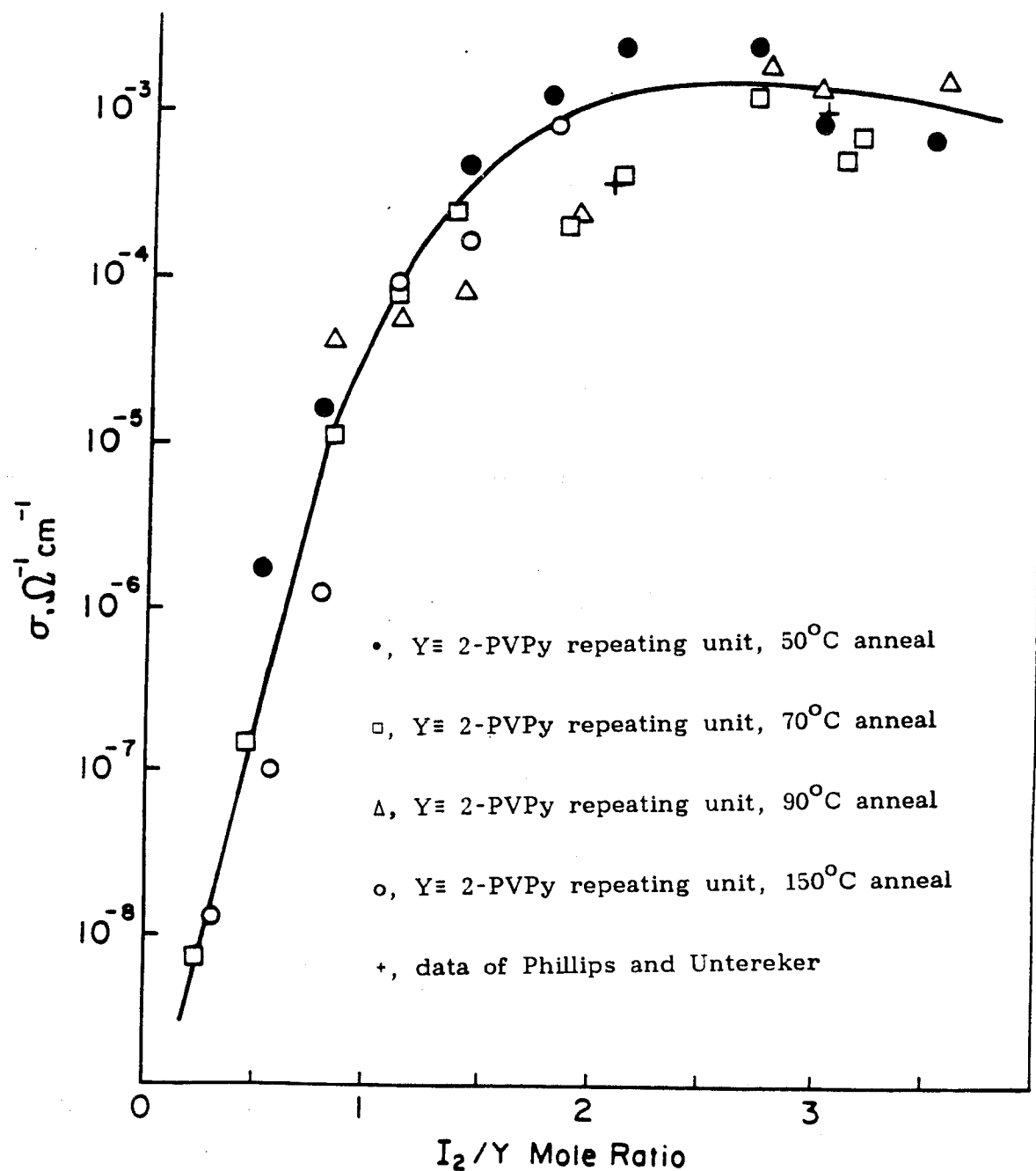


Figure 20: Variation of conductivity with iodine content

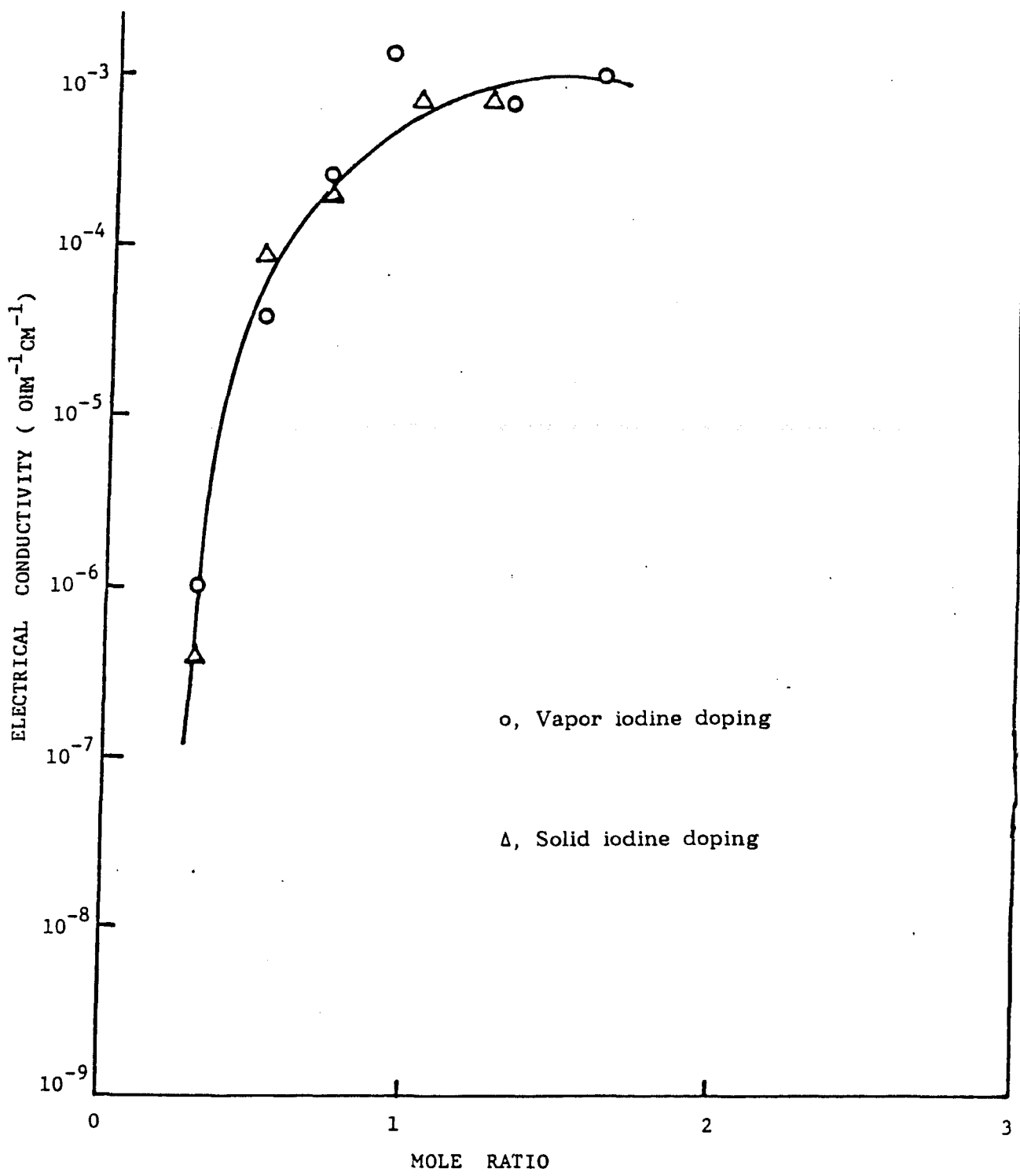


Figure 21: Comparison of conductivity of PPAN using two different doping procedures

3.2.3 Electron Spin Resonance

Electron spin resonance (ESR) spectra were obtained for 2-PVPy and PPAN with varying iodine to segment mole ratios.

Both annealed 2-PVPy and PPAN show no ESR spectra when undoped. Upon doping with iodine, both PPAN-I₂ and PVPy-I₂ show a single peak in their ESR spectra, as is shown in Figures 22 and 23, respectively. The g-factors and intensities of the signals are both seen to change with a variation in the iodine to polymer mole ratio for both polymers. There does not appear to be any clear cut quantitative relationship between the mole ratio and the intensity of the signals. Figures 24 and 25 show how the g-factor varies with changes in the iodine to segment mole ratio for 2-PVPy-I₂ and PPAN-I₂ respectively.

The ESR spectra of 2-PVPy-I₂ become more complicated for samples with an iodine to 2-PVPy segment mole ratio of 2.7 and above. Several peaks of lower intensity appear on both sides of the main peak at these mole ratios. More work is required in this area to determine the significance of the data.

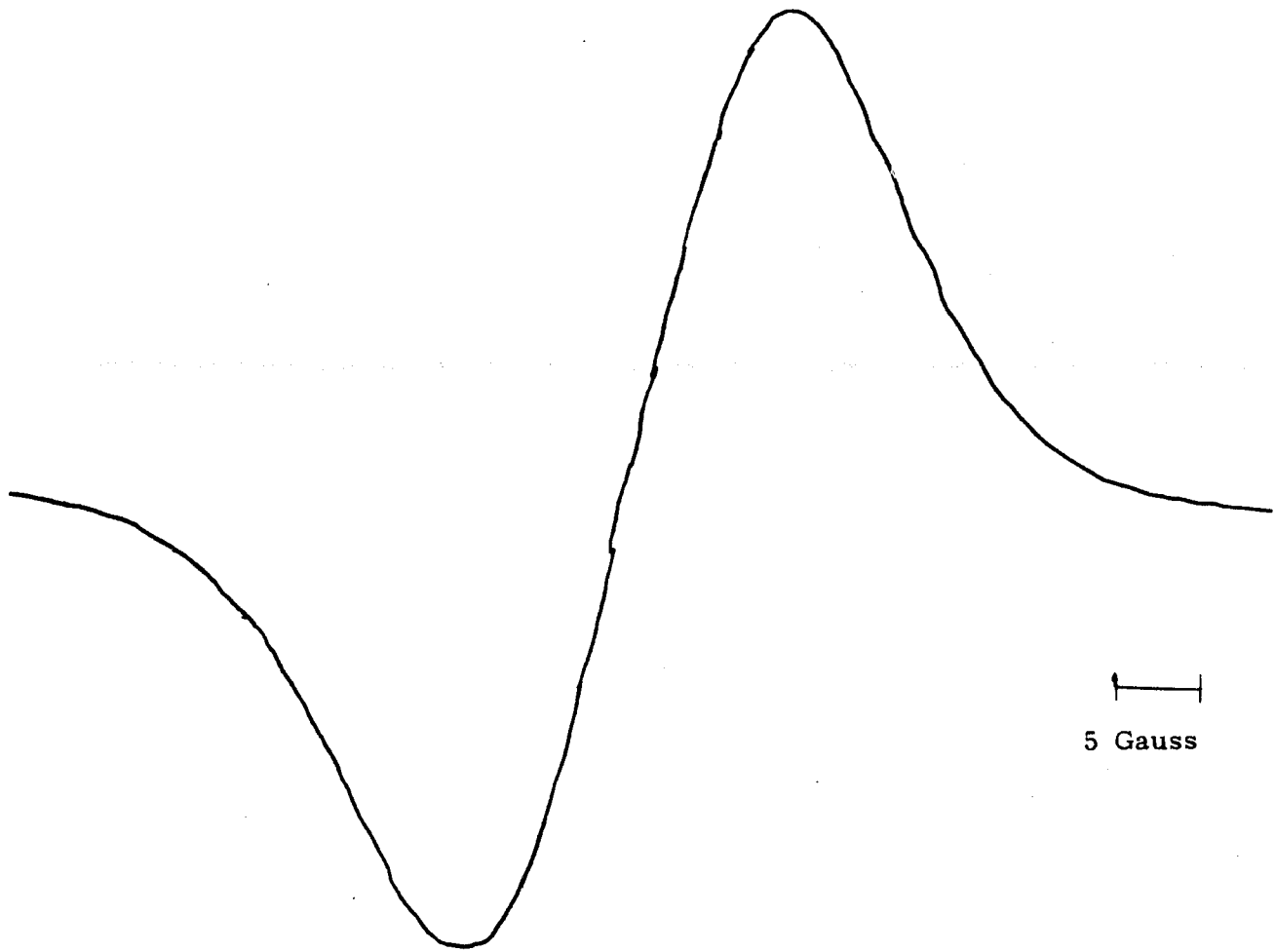


Figure 22: Electron spin resonance spectrum of PPAN-1(I₂)_{0.5}

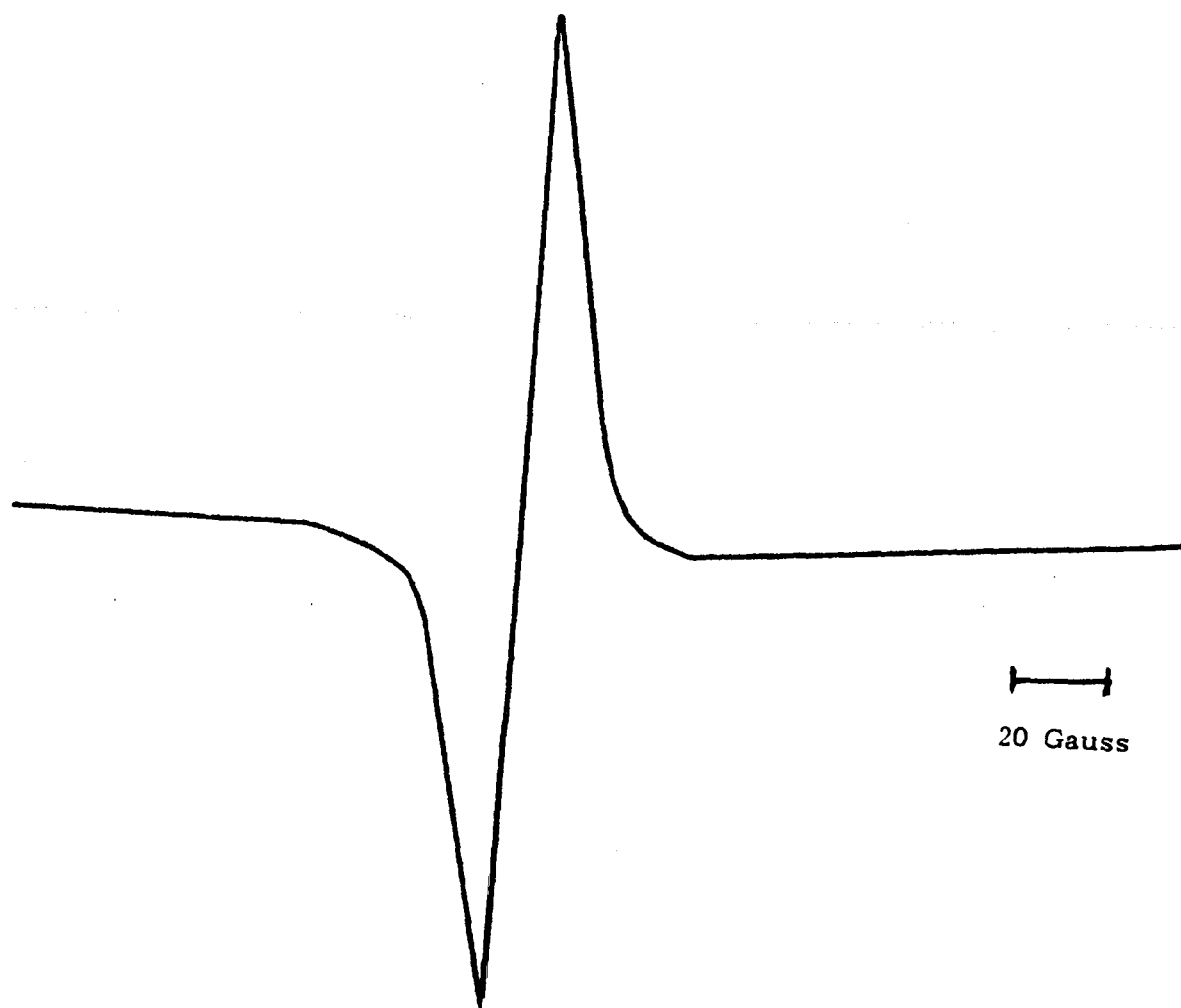


Figure 23: Electron spin resonance spectrum of 2-PVPy(I₂)_{1.1}
90°C anneal

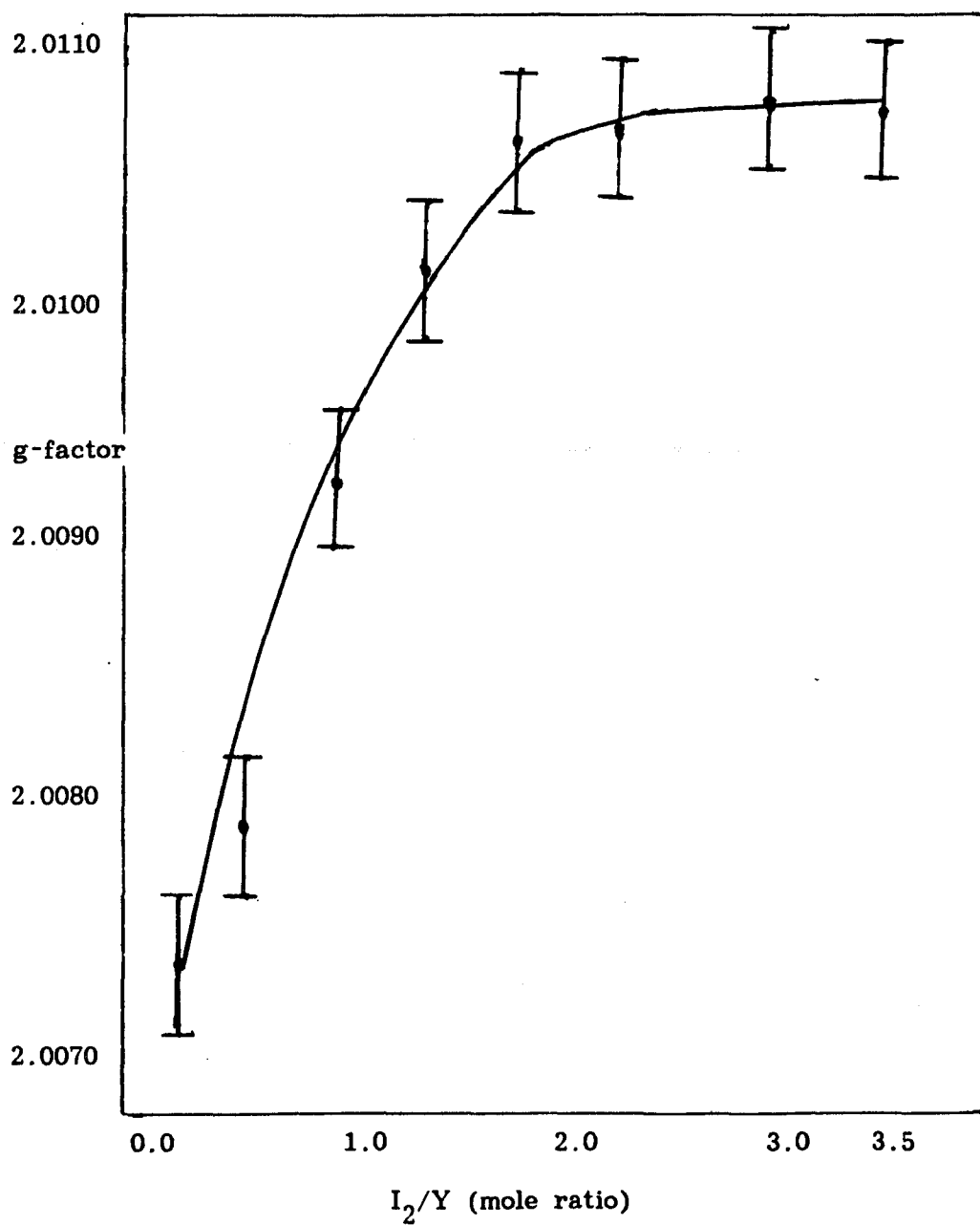



Figure 24: Variation of g-factor with iodine content for 2-PVPy


 ≡ Estimated limits of error in calculation of g-factor, ± 0030

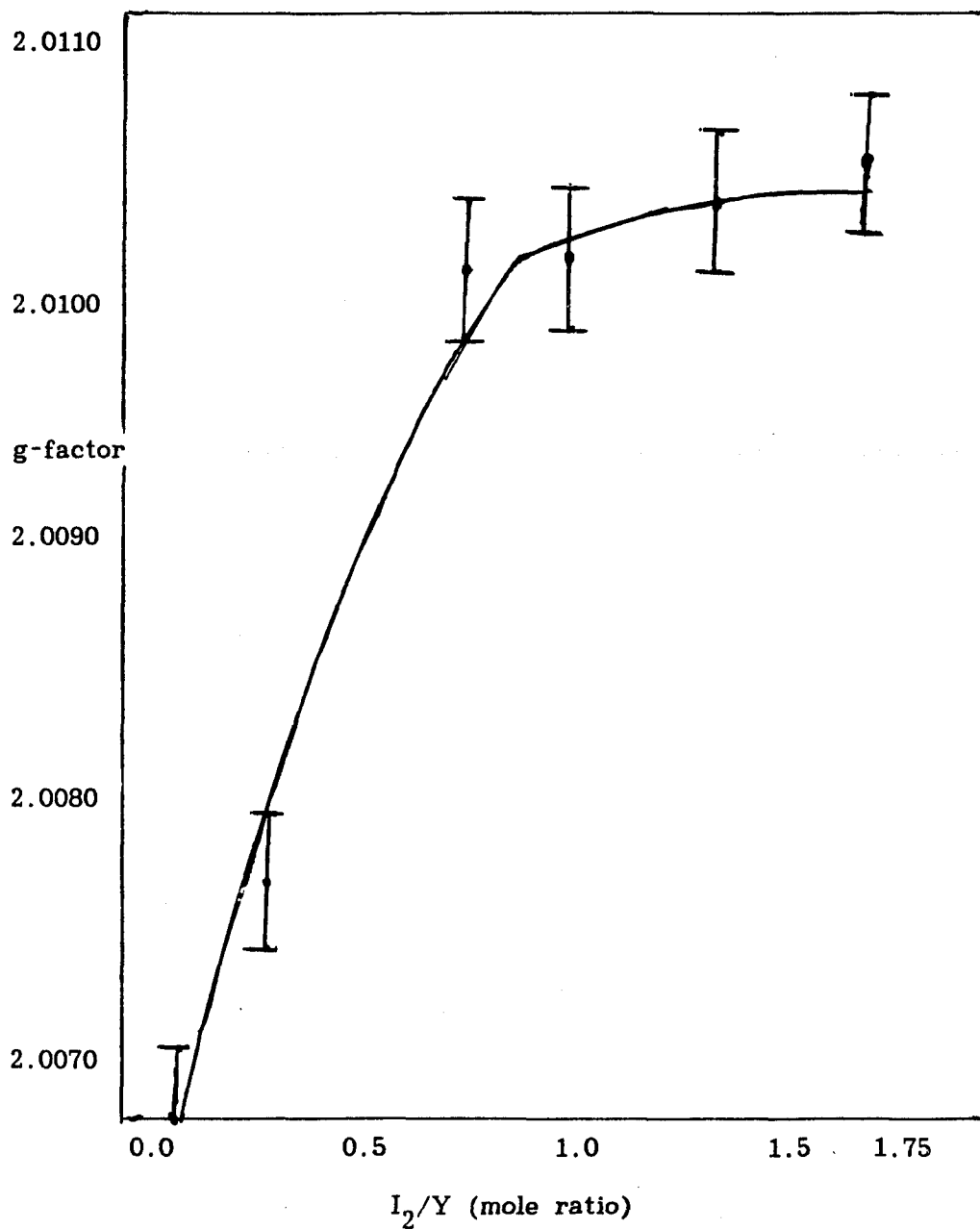


Figure 25: Variation of g-factor with iodine content for PPAN-1

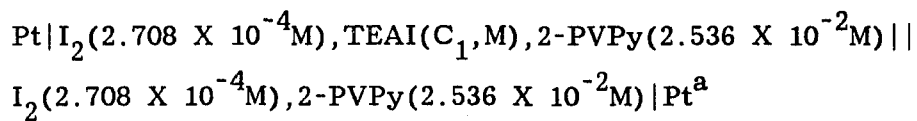


≡ Estimated limits of error in calculation of g-factor, ± 0030

Appendix A
EMF data on 2-polyvinylpyridine-iodine
in 1,2 dichloroethane solutions

TABLE 11

EMF data on the cell

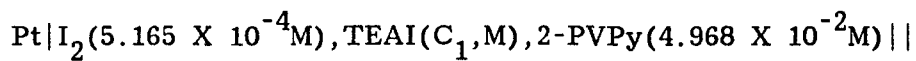


C_1 MX10 ⁵	EMF mV	Y MX10 ⁵	K' M ² X10 ⁹	X MX10 ⁵
.314	1.12	3.45	1.30	3.60
.617	2.24	3.24	1.25	3.53
.907	3.23	3.17	1.30	3.60
1.19	4.18	3.09	1.32	3.63
1.46	5.07	3.01	1.35	3.67
1.72	5.90	2.95	1.37	3.71
1.97	6.68	2.89	1.40	3.74
2.21	7.38	2.85	1.44	3.80
2.45	8.08	2.79	1.46	3.82
2.67	8.79	2.72	1.47	3.83
				3.69± .037

^aOxidation occurs on the side of the cell containing TEAI.

TABLE 12

EMF data on the cell



C_1 MX10 ⁵	EMF mV	Y MX10 ⁵	K' M ² X10 ⁹	X MX10 ⁵
.636	1.21	6.44	4.56	6.75
1.25	2.38	6.13	4.52	6.73
1.84	3.58	5.72	4.32	6.57
2.40	4.74	5.39	4.20	6.48
2.95	5.87	5.09	4.10	6.40
3.48	7.03	4.77	3.94	6.28
3.99	8.14	4.51	3.83	6.19
4.48	9.24	4.25	3.71	6.09
4.95	10.31	4.02	3.61	6.01
5.41	11.37	3.80	3.50	5.92
				6.34± .082

^aOxidation occurs on the side of the cell containing TEAI.

TABLE 13

EMF data on the cell

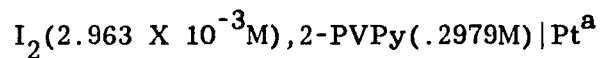
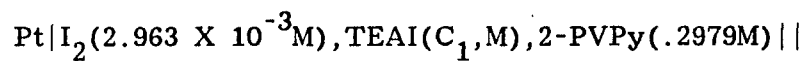
Pt|I₂(1.112 X 10⁻³M), TEAI(C₁,M), 2-PVPy(.1000M)||I₂(1.112 X 10⁻³M), 2-PVPy(.1000M)|Pt^a

C ₁ MX10 ⁵	EMF mV	Y MX10 ⁴	K' M ² X10 ⁸	X MX10 ⁴
1.24	1.20	1.37	2.09	1.44
2.43	2.45	1.35	2.22	1.49
3.57	3.59	1.33	2.34	1.53
4.68	4.81	1.28	2.38	1.54
5.74	6.00	1.21	2.35	1.53
6.76	7.10	1.14	2.26	1.50
7.75	8.06	1.09	2.21	1.49
8.71	9.01	1.04	2.16	1.47
9.63	9.99	.982	2.10	1.45
10.05	10.83	.938	2.04	1.43
				1.49± .012

^aOxidation occurs on the side of the cell containing TEAI.

TABLE 14

EMF data on the cell



C_1 $\text{MX}10^4$	EMF mV	Y $\text{MX}10^4$	K' $\text{M}^2 \times 10^8$	X $\text{MX}10^4$
.319	1.29	3.02	10.01	3.17
.625	2.53	2.87	10.00	3.17
.920	3.68	2.77	10.02	3.20
1.20	4.82	2.64	10.02	3.19
1.48	5.96	2.50	9.96	3.15
1.74	7.04	2.29	9.84	3.14
2.00	8.05	2.39	9.81	3.13
2.24	8.99	2.21	9.85	3.14
2.48	9.92	2.13	9.81	3.13
2.71	10.80	2.06	9.79	3.13
				3.16± .012

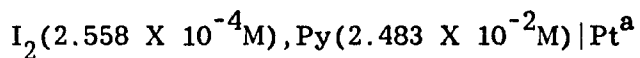
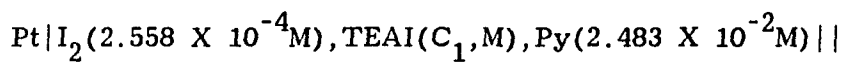
^aOxidation occurs on the side of the cell containing TEAI.

Appendix B

EMF data on pyridine-iodine in 1,2 dichloroethane solutions

TABLE 15

EMF data on the cell

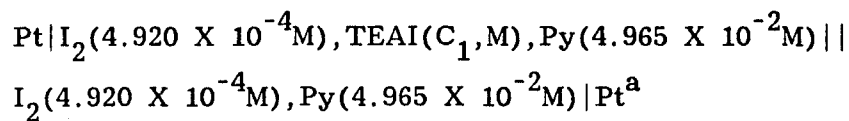


C_1 MX10 ⁵	EMF mV	Y MX10 ⁵	K' M ² X10 ¹⁰	X MX10 ⁵
.271	1.11	3.00	9.82	3.13
.531	2.15	2.92	10.01	3.17
.782	3.09	2.88	10.05	3.24
1.02	4.03	2.78	10.05	3.25
1.26	4.99	2.65	10.03	3.21
1.48	5.94	2.52	10.01	3.17
1.70	6.87	2.40	9.82	3.13
1.19	7.78	2.29	9.60	3.10
2.11	8.63	2.20	9.48	3.08
2.30	9.42	2.13	9.43	3.07
				3.16 ± .026

^aOxidation occurs on the side of the cell containing TEAI.

TABLE 16

EMF data on the cell

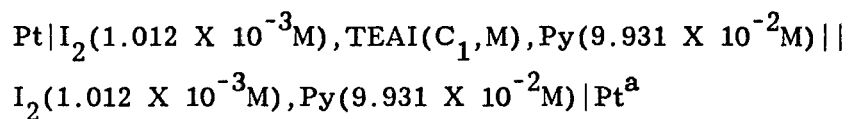


C_1 MX10 ⁵	EMF mV	Y MX10 ⁵	K' M ² X10 ⁹	X MX10 ⁵
.705	1.60	5.32	3.20	5.66
1.38	3.18	4.92	3.11	5.57
2.04	4.68	4.63	3.09	5.56
2.66	6.18	4.31	3.01	5.48
3.27	7.65	4.02	2.92	5.41
3.85	8.94	3.83	2.94	5.43
4.42	10.10	3.69	3.00	5.47
4.96	11.21	3.56	3.03	5.51
5.48	12.31	3.41	3.04	5.51
5.59	13.30	3.30	3.07	5.54
				5.51± .039

^aOxidation occurs on the side of the cell containing TEAI.

TABLE 17

EMF data on the cell

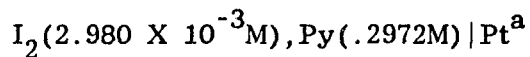
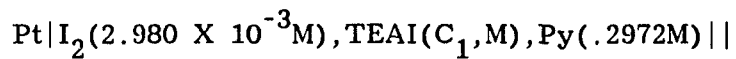


C_1 MX10 ⁵	EMF mV	Y MX10 ⁴	K' M ² X10 ⁸	X MX10 ⁴
1.20	1.27	1.15	1.17	1.21
2.36	2.50	1.18	1.46	1.21
3.47	3.65	1.06	1.48	1.22
4.54	4.93	.974	1.38	1.18
5.57	6.09	.915	1.35	1.16
6.56	7.22	.869	1.33	1.15
7.52	8.18	.843	1.35	1.16
8.45	9.10	.821	1.36	1.17
9.34	10.04	.792	1.36	1.17
10.02	10.95	.757	1.35	1.16
				1.18 ± .009

^aOxidation occurs on the side of the cell containing TEAI.

TABLE 18

EMF data on the cell



C_1 MX10 ⁴	EMF mV	Y MX10 ⁴	K' M ² X10 ⁸	X MX10 ⁴
.329	1.09	3.71	1.50	3.87
.644	2.07	3.69	1.59	4.00
.948	3.01	3.59	1.63	4.04
1.24	4.02	3.38	1.56	3.95
1.52	5.06	3.16	1.48	3.84
1.80	6.09	2.96	1.41	3.75
2.06	7.10	2.79	1.35	3.68
2.31	8.08	2.64	1.31	3.61
2.56	9.04	2.50	1.27	3.56
2.79	9.91	2.40	1.25	3.53
				3.78± .051

^aOxidation occurs on the side of the cell containing TEAI.

REFERENCES

1. Audrieth, L.F.; Birr, E.J. J. Am. Chem. Soc. 1933, 55, 668.
2. Reid, C.; Mulliken, R.S. J. Am. Chem. Soc. 1954, 76, 3869.
3. Kortum, G.; Wilski, H. Z. Physik. Chem. 1953, 202, 35.
4. Zingaro, R.; Vander-Werf, C.A.; Kleinberg, J. J. Am. Chem. Soc. 1951, 73, 88.
5. Pezzatini, G.; Guidelli, R. Electrochim. Acta 1971, 16, 1415.
6. Nigretto, J.M.; Josefowicz, M. Electrochim. Acta 1974, 19, 809.
7. Nigretto, J.M.; Josefowicz, M. "Pyridine as a Nonaqueous Solvent" in Lagowski, J.J. Ed.; "The Chemistry of Nonaqueous Solvents" Academic Press, 1978, Chapter 5.
8. Aronson, S; Epstein, P; Aronson, D.B.; Wieder, G. J. Phys. Chem. 1982, 86, 1035.
9. Lerner, N.R. Polymer, 1983, 24, 800.
10. McKinney, W.J.; Wong, M.K.; Popov, A.I. Inorg. Chem. 1968, 7, 1001.
11. Van Braam Houckgeest, J.P.W.A. Rect. Trav. Chim. 1941, 60, 433.
12. Popov, A.I.; Swensen, R.F.; J. Am. Chem. Soc. 1955, 77, 3724.
13. Yeh, T.I. Thesis, City University of New York, 1984.
14. McKinney, W.J.; Popov, A.I. J. Am. Chem. Soc. 1969, 91, 5215.
15. Wagner, C. "Thermodynamics of Alloys" Addison- Wesley, 1952, p. 12.
16. Aronson, S.; Katlowitz, N. J. In. Nucl. Chem. 1979, 41, 1579.
17. Phillips, G.M.; Untereker, D.F. Proceedings of the 29th Power Sources Symposium 1980, p. 195, published by the Electrochemical Society, Princeton, N.J.

18. Buckles, R.E.; Yuk, J.P.; Popov, I.A. J. Am. Chem. Soc. 1952, 74, 4379.
19. Van der Pauw, L.J. Phillips Tech. Rev. 1958, 20, 320.
20. Mulliken, R.S. J. Phys. Chem. 1952, 56, 810.